The importance of burning conditions on the composition of domestic biomass burning organic aerosol and the impact of atmospheric aging

Rhianna L. Evans[1], Daniel J. Bryant[1], Aristeidis Voliotis[2,3], Dawei Hu[2], HuiHui Wu[2], Sara Aisyah Syafira[2], Osayomwanbor E. Oghama[2], Gordon McFiggans[2], Jacqueline F. Hamilton[1,4], and Andrew R. Rickard[1,4]

[1]Wolfson Atmospheric Chemistry Laboratories, Department of Chemistry, University of York, York, YO10 5DD
[2]Centre for Atmospheric Science, Department of Earth and Environmental Sciences, School of Natural Sciences, University of Manchester, Manchester, M13 9PL
[3]National Centre for Atmospheric Science, University of Manchester, Manchester, M13 9PL
[4]National Centre for Atmospheric Science, University of York, York, YO10 5DD

Correspondence: Jacqueline F. Hamilton (jacqui.hamilton@york.ac.uk) and Andrew R. Rickard (andrew.rickard@york.ac.uk)

Abstract. Domestic biomass burning is a significant source of organic aerosol (OA) to the atmosphere however the understanding of OA composition under different burning conditions and after oxidation is largely unknown. Compositional analysis of OA is often limited by the lack of analytical standards available for quantification, however, semi-quantitative non-target analysis (NTA) can overcome these limitations by enabling the detection of thousands of compounds and quantification via surrogate standards. A series of controlled burn experiments were conducted at the Manchester Aerosol Chamber to investigate domestic biomass burning OA (BBOA) under different burning conditions and the impact of atmospheric aging. Insights into the chemical composition of fresh and aged OA from flaming dominated and smouldering dominated combustion were obtained via a newly developed semi-quantitative NTA approach using ultra-high-performance liquid chromatography high-resolution mass spectrometry. Aerosol from smouldering dominated burns contained significant organic carbon content whereas under flaming dominated conditions was primarily black carbon. The detectable OA mass from both conditions was dominated by oxygenated compounds (CHO) ($\approx$ 90 %) with smaller contributions from organonitrogen species. Primary OA (POA) had a high concentration of C_8-C_{17} CHO compounds with both burns exhibiting a peak between C_8-C_{11}. However, flaming dominated POA exhibited a greater contribution of C_{13}-C_{17} CHO species. More than 50 % of the CHO mass in POA was determined as aromatic by the aromaticity index, largely in the form of functionalised monoaromatic compounds. After aging the aromatic contribution to the total CHO mass decreased with a greater loss for smouldering (-53%) than flaming (-16 %) due to the increased reduction of polyaromatic compounds under smouldering conditions. The O:C ratios of the aged OA from flaming and smouldering were consistent with those from the oxidation of aromatic compounds (0.57 - 1.00), suggesting that compositional changes upon aging were driven by the oxidation of aromatic compounds and the loss of aromaticity. However, there was a greater probability of O:C ratios $\geq$ 0.8 in aged smouldering OA indicating the presence of more oxidised species. This study presents the first reported quantitative non-target compositional analysis of domestic BBOA using retention window scaling

and demonstrates compositional changes between burn phase and after aging may have important consequences for exposure to such emissions in residential settings.

1 Introduction

Biomass burning (BB) encompasses a range of combustion processes such as wildfires, agricultural burning, and domestic combustion of solid fuels or referred to herein, domestic BB. Biomass burning is one of the largest sources of organic aerosol (OA) and trace gases to the atmosphere, emitting approximately 62 Tg yr^{-1}, 77 Tg yr^{-1} and 19 Tg yr^{-1} of volatile organic compounds (VOCs), particulate matter less than 2.5 μm in diameter (PM$_{2.5}$) and nitrogen oxides (NO$_x$) respectively to the atmosphere (Andreae, 2019). Biomass burning VOCs (BBVOCs) can oxidise in the atmosphere leading to the production of secondary organic aerosol (SOA) which is a major component of PM$_{2.5}$. With respect to human health, PM$_{2.5}$ is a highly toxic air pollutant as fine particles can be inhaled deep into the respiratory tract (Kampa and Castanas, 2008). Approximately 2 billion people globally use solid fuels for heating and cooking (World Bank, 2024) representing a chronic exposure to poor air quality and annually solid fuel combustion is responsible for 3.2 million deaths worldwide (World Health Organisation (WHO), 2022). However it was estimated that 20 % of the global annual deaths caused by PM$_{2.5}$ could be avoided by eliminating domestic BB (McDuffie et al., 2021). In the UK, approximately 8 % of the population burn wood indoors (Department for Environment Food & Rural Affairs (DEFRA), 2020) and in London solid fuel emissions comprised approximately 7-9% of PM$_{2.5}$ emissions during 2022 (Casey et al., 2023) and 26% of total primary OA (POA) during cold weather conditions consistent with domestic heating activity (Allan et al., 2010). Domestic BB is predicted to grow due to numerous energy crises in recent years and as a cheaper alternative to gas (International Energy Agency, 2022) in the rising costs of living. However, emissions from wood burning are highly dependent on combustion conditions, the fuel burnt, and the stove appliance used (Andrew Price-Allison, 2022).

A full burn cycle consists of multiple stages i) ignition, ii) flaming combustion and iii) smouldering combustion (Andreae and Merlet, 2001). During flaming the lignocellulosic biomass is partially or completely burned and char is produced, typically occurring at high temperatures. Whereas smouldering occurs during the latter stages of the burn cycle at lower temperatures, starting once all the combustible volatile fuel is consumed and the oxidation of char begins (Andreae and Merlet, 2001). Due to these unique conditions a characteristic mixture of VOC emissions arises at each stage from temperature dependent pyrolysis mechanisms at varying abundances (Andreae and Merlet, 2001; Czech et al., 2016; Liu et al., 2017; Stewart et al., 2021). For instance, Czech et al. (2016) observed the greatest emissions from the ignition phase followed by ember (smouldering) and stable burn (flaming) phases. Previously the change in emissions between burn phase was identified using positive matrix factorisation which separated BBVOC emissions into two factors; low and high temperature combustion. Low temperature combustion contained more oxygenated aromatics and furanic compounds in agreement with particle phases enriched in

oxygenated organic compounds from smouldering combustion (Sekimoto et al., 2018; Weimer et al., 2008). In contrast, BB-VOCs from high temperature combustion consisted of polyaromatic hydrocarbons (PAHs), terpenes and aliphatic unsaturated hydrocarbons (Sekimoto et al., 2018; Stefenelli et al., 2019).

55   Ultra-high-performance liquid chromatography coupled to electrospray ionisation high-resolution mass spectrometry (UHPLC-ESI-HRMS) is a valuable technique for studying the composition of OA enabling the detection of thousands of compounds and separation of isomeric species. Various tracer species from biomass burning OA (BBOA) have been previously identified using UHPLC-HRMS (e.g., Claeys et al., 2012; Kourtchev et al., 2016; Budisulistiorini et al., 2017; Iinuma et al., 2007; Capes et al., 2008; Daellenbach et al., 2019; Brege et al., 2018; Wang et al., 2017b; Smith et al., 2020; Zangrando et al., 2013), but

60   most commonly consisted of levoglucosan and nitroaromatic compounds (NACs) (Claeys et al., 2012; Kourtchev et al., 2016; Budisulistiorini et al., 2017; Iinuma et al., 2010; Piot et al., 2012; Kitanovski et al., 2012; Li et al., 2017). Biomass burning plumes are ideal conditions for NAC formation due to high emissions of NO_x and aromatic VOCs from lignin degradation which is primarily comprised of 3 aromatic alcohol units; coumaryl, sinapyl and coniferyl alcohol (Simoneit et al., 1993). In particular NACs such as nitrophenols are widely adopted as tracers due to strong correlations with levoglucosan (Iinuma

65   et al., 2010; Jiang et al., 2020; Cai et al., 2022) and depending on the fuel type emission factors range between 1.4 - 31 mg kg^{-1} (Iinuma et al., 2007, 2010; Claeys et al., 2012; Kourtchev et al., 2016). These compounds also have important climatic impacts by contributing to brown carbon (BrC) hence their extensive study in the wider literature (Fleming et al., 2020; Zhou et al., 2022; Wang et al., 2020; Lin et al., 2016; Gilardoni et al., 2016). However, by selecting a small number of compounds to analyse, limited compositional information can be obtained by targeted approaches, for instance, Pereira et al. (2021) estimated

70   only 1.1% of the mass of an ambient OA filter could be quantified via a targeted approach using 60 authentic standards.

Non-target analysis (NTA) can overcome these limitations by enabling chemical information, such as molecular formula, of all detected analytes within a complex mass spectral output to be rapidly obtained. For example, NTA enabled the identification of 190 NACs in $PM_{2.5}$ from Beijing, with a third attributed to biomass burning (Wang et al., 2021). Furthermore, species associated with lignin pyrolysis such as vanillin, coniferaldehyde and benzoic acid and sugars including levoglucosan, sucrose

75   and fructose from cellulose degradation were previously identified in BBOA via NTA approaches (Simoneit, 2002; Smith et al., 2020, 2009). However, due to the lack of commercially available authentic standards many previous NTA studies used limited metrics such as number of molecular formulas or peak area to estimate relative abundance (eg., Dzepina et al., 2015; Wang et al., 2020; Brege et al., 2021; Smith et al., 2009; Pereira et al., 2021; Brege et al., 2018; Herrera-Lopez et al., 2014). The lack of standardised metrics to estimate abundance can lead to differences in inferred composition. Using peak area, Wang

80   et al. (2020) and Brege et al. (2018) observed a large quantity of organonitrogen compounds (CHON) in OA during periods influenced by biomass burning, which were attributed to NACs. In contrast, using the number of formulas showed a greater contribution of oxygenated organic compounds (CHO) in BBOA (Brege et al., 2021; Dzepina et al., 2015; Smith et al., 2009). For example, at the Pico Mountain Observatory in the North Atlantic, analysis of $PM_{2.5}$ samples showed CHO compounds accounted for 70 % of the molecular assignments in air masses influenced by wildfires (Dzepina et al., 2015) and Smith et al.

85   (2009) observed CHO compounds represented 80-90% of all detected mass spectral features in BBOA.

Whilst the number of formulas can provide some information on sample complexity, it is not quantitative for concentration, and although peak area is often considered as quantitative neither of these approaches accounts for differences in ionisation efficiency (IE) between different species. IE is a measure of the ability of a species to ionise within an ESI source and is highly structurally specific, varying by multiple orders of magnitude between different compounds including amongst structural isomers (Oss et al., 2010; Liigand et al., 2021). For instance, across isomers of methyl-nitrophenol ($C_7H_7NO_3$) IE can vary by 3 orders of magnitude (Evans et al., 2024). Therefore, improved NTA methodology incorporates quantification into the workflow. These approaches have largely quantified compounds with known structures through the use of predictive models which predict the IE of a structurally identified compound relative to that of a reference compound, known as the relative ionisation efficiency (RIE) (Bryant et al., 2023; Liigand et al., 2021; Mayhew et al., 2020). However, the quantification of unidentified compounds remains a challenge. Sepman et al. (2023) recently developed a model using fragmentation mass spectra (MS^2) to obtain molecular fingerprints of unknown species for the prediction of IE. Often NTA UHPLC-HRMS approaches use data-dependent MS^2 (ddMS^2) to obtain higher quality MS^2 (Guo and Huan, 2020) which means only a certain number of species are selected for fragmentation in each scan. Therefore, relying on MS^2 for quantification means some compositional information is lost. For example, using a NTA workflow Wang et al. (2022) observed only 39% of detected compounds had MS^2 spectra using ddMS^2. Alternative methods for the quantification of unknowns without MS^2 involves semi-quantification using a singular structurally similar surrogate standard which is assumed to have a similar IE to the target compound (Kim et al., 2023a; Kruve et al., 2021; Pieke et al., 2017; Rattanavaraha et al., 2016; Wang et al., 2023). A recent methodology outlined in Evans et al. (2024) enabled the quantification of all unidentified species by using the average IE of multiple surrogate standards which elute within the same retention time window as the unknown analytes. The coupling of retention time and chemical functionality in this methodology enabled quantification by chemically and structurally similar compounds, and therefore, more reliable estimates of concentration with uncertainties.

In this study, chamber experiments were conducted at the Manchester Aerosol Chamber (MAC) to investigate the effect of combustion conditions on the chemical composition of fresh OA emitted from domestic wood burning and the subsequent aged OA. Using a domestic wood burning stove, emissions during burn phases dominated by smouldering or flaming were sampled and subsequently photochemically aged inside an atmospheric simulation chamber. UHPLC-HRMS in negative mode ESI was used to analyse the chemical composition of OA formed from different burn phases in fresh and aged emissions. Overall, this study presents the first molecular level semi-quantitative NTA of domestic BBOA improving our understanding of the prominent species contributing to domestic BBOA under different burn phases and the compositional changes occurring after atmospheric aging. These findings aim to aid future policy on the mitigation of poor air quality, climatic impacts and the harmful health effects from domestic BB.

2 Methodology

2.1 Controlled burn chamber experiments

2.1.1 Design

Controlled burn chamber experiments were conducted over two campaigns during April 2022 and September 2022 at the Manchester Aerosol Chamber (MAC) located at the University of Manchester, UK. The experiments aimed to investigate the aerosol composition under different burning conditions. $PM_{2.5}$ filter samples were taken for detailed offline composition analysis and a large suite of online instrumentation measured aerosol composition, aerosol physical properties and trace gases, including carbon monoxide (CO), carbon dioxide (CO_2), ozone (O_3) and NO_x. The MAC has previously been described in detail elsewhere (Shao et al., 2022). However, in brief the MAC consists of an enclosed and suspended 18 m^3 fluorinated ethylene Teflon bag supported by 3 rectangular aluminium frames, where the outer frames move freely allowing the bag to expand or contract when filling or emptying the chamber. The chamber was illuminated using two 6 kw xenon arc lamps with quartz fibre glass filters and 4 rows of halogen lamps (64 bulbs) to simulate atmospheric solar wavelengths, which enables the photolysis of NO_2 to produce O_3. O_3 is then subsequently photolysed in the presence of water molecules to produce OH (Voliotis et al., 2021, 2022a; Shao et al., 2022). Heterogeneous wall chemistry will also produce HONO, which is photolysed to yield OH and NO. The OH concentration inside the MAC has been previously calculated as ca. 1×10^6 molecules cm^{-3} (Voliotis et al., 2021, 2022b) at similar NO_x concentrations to these experiments. Purified dry air was supplied to the chamber by passing laboratory air through a 3-phase blower and 3 filters comprising i) purafil/charcoal mixture, ii) charcoal and iii) HEPA. The chamber had automated fill/flush cycles before and after experiments, detailed in Shao et al. (2022), to reduce the chamber background signal and was cleaned overnight with high concentrations of O_3 ($\approx$ 1ppm) to oxidise any residual species. A cleaning programme was performed once a week by illuminating the chamber for 4-5 hours under high O_3 concentrations ($\approx$ 1ppm). During the controlled burn campaigns multiple background experiments were conducted whereby a clean chamber, ie. no added smoke from the stove, was irradiated with light for 6 hours. After this time, a filter sample was collected of the chamber air via the flush line at approximately 3 m^3 min^{-1} for 4 minutes.

For the controlled burn experiments, hardwood (Beech), which typically provides more heat and burn for longer than softwood, was burnt in a Ecodesign stove (Esse Model 175 F) to represent a typical domestic fuel in the UK. The emissions from the burn were sampled during flaming or smouldering phases. However given the nature of a burn which will be composed of both flaming and smouldering processes it is difficult to separate distinct phases therefore the burns are referred to herein as "flaming dominated" and "smouldering dominated". The catalytic filter within the stove, which would enable the "particulate reburn" technology to reduce particulate emissions beyond that of the UK Ecodesign requirements, was removed to replicate more conventional stoves in the UK market. The wood smoke from the flue derived from either smouldering or flaming dominated phases (2 L min $^{-1}$) was then diluted with a flow of compressed air (2 L min^{-1}) before injection into the chamber using an eDiluter (eDiluter Pro, Dekati, Finland). The smouldering dominated phase was controlled by allowing the wood to be consumed by flames and subsequently closing the stove ventilation to reduce the presence of oxygen in the stove. Injection

of the stove emissions into the chamber started when there was a lack of visible flames. No additional reactants were injected into the chamber. The injection of the stove emissions proceeded until the total particle mass concentration measured in the chamber was twice the target concentration at half the chamber volume. Then the final addition of scrubbed particle free air into the bag achieved the target concentration of around 200 μg m^{-3} at full chamber volume. Due to the relatively low particle concentration of 200 μg m^{-3} inside the chamber the fresh aerosol was sampled directly from the flue of the wood burner to yield sufficient mass for offline chemical composition analysis rather than from the chamber itself. POA was sampled from the flue at 2 L min^{-1} for 5 minutes. Following injection of the stove emissions, 40-60 minutes of background data was collected to allow instrumentation with long cycle times to obtain several cycles of data. After this period the chamber was irradiated producing OH radicals for photo-oxidation and the stove emissions aged for approximately 6 hours. The relative humidity throughout the experiment was controlled between 50-60 % and the temperature inside the chamber was kept around 25 °C. At the end of the 6 hour experiment, an aged filter sample was taken by evacuating the contents of the chamber onto a pre-baked Quartz filter for 4 minutes. The exact flow rate of the vacuum line for collection was not directly measured, however, the MAC can be completely flushed from full in approximately 6 minutes, therefore, the flow rate is approximated as 3 m^3 min^{-1} (Shao et al., 2022). Quartz filters (Whatman QMA, 47mm) used for sample collection were individually wrapped in foil and pre-baked at 500 °C for 5 hours prior to use. After collection the filters were wrapped in the pre-baked foil, transported on ice to the University of York and finally stored at -20 °C before offline analysis.

Each aging experiment, where aging is defined as being both photo-oxidative and dilution processes as would occur in the atmosphere upon emission from stoves, was repeated once. This resulted in two sample types per burn phase, fresh and light aged, with one filter for the fresh emissions and two filters for the aged experiments. However, as previously stated in practice the fire can be undergoing flaming and smouldering phases at the same time meaning it can be difficult to exactly separate a singular phase into the chamber. As such one of the repeats aiming to capture the smouldering dominated phase was characterised as an intermediary burn with increased flaming characteristics, ie. high CO_2 concentrations, but also exhibiting high ratios of organic:black carbon (OC:BC) associated with smouldering. This experiment is not discussed further in this study. The experiments, their sample ID referred to in this study and initial concentrations of gas and particle phase species before aging are presented in Table 1.

2.1.2 Online Instrumentation

The experiments used a variety of online instrumentation to monitor the evolving aerosol and gaseous composition throughout the photo-oxidation of the wood burning smoke inside the MAC. Non-refractory PM$_1$ composition was measured via a high-resolution-time-of-flight aerosol mass spectrometer (HR-ToF-AMS) enabling real-time measurements of NH_4^+, NO_3^-, Cl^-, SO_4^{2-} and the organic fraction. The extent of oxidation could be monitored using the fraction of the 44 *m/z* fragment compared to the total organic fraction (f$_{44}$) with higher f$_{44}$ levels associated with more oxygenated organic aerosol. Whilst the signal at *m/z* 60 has been associated as a fragment from biomass burning tracers such as levoglucosan and other structurally similar sugars. Therefore, the degradation of the wood smoke throughout photo-oxidation was also monitored using the fraction of *m/z* 60 to the total organic fraction (f$_{60}$). Additionally, particle concentrations were measured using a Scanning Mobility Particle

Table 1. List of the OA samples used in this study and the initial conditions at the start of the aging period

Experiment date	Conditions	Sample ID	Aging period / hrs	PM concentration / μg m^{-3}	NO:NO$_2$	OC:BC*	MCE
21/04/2022	Flaming light aged	FL_AGED_1	5:50	243.6	1.94	0.32	0.96
26/04/2022	Smouldering light aged	SM_AGED	6:05	213.6	1.81	406.3	0.78
28/04/2022	Flaming light aged	FL_AGED_2	6:05	153.4	3.74	0.21	0.93
30/08/2022	Flaming fresh flue	FL_FRESH	-	-	-	-	-
31/08/2022	Smouldering fresh flue	SM_FRESH	-	-	-	-	-

*OC refers to the total organic content measured by AMS

Sizer (SMPS) across a size range of 10-700 nm and measurements of black carbon mass and coating thickness were obtained from a Single Particle Soot Photometer (SP2).

2.1.3 Offline Instrumentation

Prior to offline analysis the filters were extracted based on the method used in Bryant et al. (2023). The 47 mm quartz filters were cut into 1 cm^2 pieces, placed in a 20 mL glass vial and 10 mL of methanol (LC-MS Optima Grade) was added. For fresh aerosol samples half a 47mm filter was used due to the higher aerosol mass loading. The resulting 10 mL solution was sonicated for 45 minutes, using ice packs to lower the temperature of the water bath. The methanol extract was transferred to a second 20 mL glass vial using a 0.22 μm syringe filter (Milipore) then dried using a Genevac vacuum solvent evaporator. The sample was reconstituted in 200 μL 90:10 H$_2$O (LC-MS Optima Grade): MeOH (LC-MS Optima Grade) for UHPLC-HRMS analysis.

The offline filters were characterised at the University of York using an Ultimate 3000 UHPLC (Thermo Scientific, USA) coupled to a Q Exactive Orbitrap MS (Thermo Fisher Scientific, USA) with heated electrospray ionisation (HESI) enabling high resolution and detailed chemical information to be obtained. Compound separation was achieved using a reversed phase C$_{18}$ 2.6 μm x 2.1 mm x 10 mm Accucore column held at 40 °C. The mobile phase consisted of 0.1 % (v/v %) formic acid (Acros Organics) in water (A, LC-MS Optima Grade) and methanol (B, LC-MS Optima Grade). A gradient elution was used, starting at 90 % (A) with a 1 minute post injection hold, decreasing to 10 % (A) at 26 minutes before returning to the starting conditions at 28 minutes. A final 2 minute hold at 10 % (A) allowed to the column to re-equilibrate. The flow rate was set to 0.3 mL min^{-1} and prior to analysis samples were stored in an autosampler tray at 4 °C. The injection volume was set to 4 μL, however injection volumes up to 10 μL were used for lower concentration samples. The HESI was operated under the following conditions: a spray voltage of 4 kV, a capillary and auxiliary gas temperature of 320 °C, a sheath gas flow rate of 45 (arb.) and an auxiliary gas flow rate of 10 (arb.) Spectra were acquired in negative and positive mode using ddMS^2 however this study only considers those acquired in negative mode. This is because of the greater sensitivity of positive mode meaning

there are a greater number of compound functionalities that can be detected which requires a significant amount of analytical standards to estimate IE. Whereas the negative mode is more selective requiring analytical standards of fewer functionalities to develop the semi-quantitative methodology. The scan range was set to a mass-to-charge ratio (*m/z*) of 85 to 750, with a mass resolution of 140,000. Tandem mass spectrometry was performed using a higher collision dissociation with a stepped normalised collision energy of 10, 20 and 45. In each scan the 10 most abundant species were selected for MS^2 fragmentation. The wood burning samples were analysed once with solvent blanks and chamber blanks analysed at the start of the sequence for blank subtraction in post-processing.

2.2 Semi-quantitative non-target analysis

Spectra were acquired from XCalibur 4.3 (Thermo Scientific, USA) and analysed using a semi-quantitative non-target workflow developed by Evans et al. (2024) for analytes detected in negative mode. In brief this method uses a non-target workflow developed in MZmine 2.53 and MZmine 3.9.0 software to detect features (Pluskal et al., 2010; Schmid et al., 2023), assign molecular formulas, and identify compounds via a spectral library search. The post processing proceeds in the following steps i) selection of the best predicted formula, ii) blank subtraction and iii) removal of data which ionised better (ie.larger peak area) in positive mode ESI and iv) semi-quantification of all detected analytes. For i) the formula with the lowest mass tolerance in ppm was chosen as the "best" formula if within the elemental ratios: 0.5 < H:C < 3, 0.05 < O:C < 2, N:C < 1, S:C < 0.5 and Cl:C < 0.2. For ii) common species detected in the sample and filter blank or chamber blank were removed if the sample-to-blank signal was < 10 and species in the wood burning samples were removed if the signal-to-noise ratio was < 3. In the final step iv) quantification is achieved via closely eluting surrogate standards for each chemical group (ie CHO, CHON, etc.). The acquired chromatogram from the UHPLC-HRMS method was split into retention time windows and authentic standards and sample analytes were assigned to a window based on their retention time and chemical group. For CHO the number of standards allowed retention time windows of 1 minute from 0 - 14 minutes and windows of 2 minutes from 16 - 20 minutes resulting in 17 retention time windows. For CHON retention time windows range between 2-3 minutes due to the lower number of available standards resulting in 8 retention time windows. Overall this methodology uses 110 standards across the retention time windows to derive average scaling factors used in quantification. A scaling factor was obtained for each retention time window by calculating the median calibration slope across the authentic standards present within each window. The list of standards used and corresponding slopes can be found in Evans et al. (2024) however, it is important to note that the slopes are instrument specific. For CHO species these slopes were predominantly derived from organic acids and for CHON species the method uses nitroaromatic standards as these are compounds likely to be observed in BBOA and are selective to negative mode ESI. Whilst for sulfur containing species (eg. CHOS, CHOSN etc) due to the lack of authentic standards a single compound, camphorsulfonic acid, is used for quantification. For the unidentified compounds, quantification is achieved via the scaling factor for the corresponding retention time window. Whereas for the compounds identified by the spectral library, quantification is achieved using an authentic standard. The semi-quantitative methodology had a relatively low quantification error of 1.52 times compared to quantification using authentic standards across 27 identified compounds in the domestic BBOA dataset characterised in this study (Evans et al., 2024).

3 Results

 ### 3.1 Insights into the oxidation of organic aerosol from online measurements

Emissions from domestic BB under different burning conditions, ie. flaming dominated or smouldering dominated, were photo-oxidised inside the MAC to observe the impact of atmospheric aging on the chemical composition of domestic BBOA. The particulate emissions from flaming dominated or smouldering dominated burn phases show that flaming is primarily formed of BC whereas smouldering shows significantly higher concentrations of OC, measured in this study as the total organic content from AMS (Fig. A1) which could impact the particle morphology (Leskinen et al., 2014) and thereby the aging of OA. The photo-oxidation of domestic BBOA was monitored in real time with an AMS to gain insight into the evolving organic fraction of non refractory PM_1 alongside instrumentation to measure the concentrations of trace gases such as nitrogen oxides (NO_x = $NO + NO_2$) (Fig. A2a). Figure 1 shows the relationship between f_{44}, representing oxidised components, and f_{60}, indicative of the levoglucosan-like species typically used as tracers of BB, over the course of the experiment and generally exhibits a negative trend of f_{60} with increasing f_{44}. This trend therefore indicates the components of the fresh BB emissions are undergoing various aging processes, due to the reduction in f_{60}, including chemical oxidation to form more oxidised species as indicated by the increase in f_{44}. However the negative correlation with f_{60} shown in Fig. 1 varies between the emissions from flaming and smouldering dominated experiments indicating the composition and atmospheric aging of OA is impacted by the burning conditions. This was similarly observed in a study investigating solid fuel emissions in London which associated two factors derived by positive matrix factorisation with two distinct f_{44} and f_{60} spaces arising from differences in burning phase or fuel type (Young et al., 2015). The increase in f_{44} ranges between 0.065 - 0.08 depending on the burn phase which is similar to the increase in f_{44} observed by Brege et al. (2018) (+0.055) between fresh and aged ambient BBOA. For the flaming dominated emissions the reduction in f_{60} is considerably less (-0.0006-0.0013) than the smouldering dominated phase (-0.025). This could be a result of reduced levoglucosan emissions during the flaming phase (Lee et al., 2010; Shafizadeh, 1982). The observed range of f_{44} and f_{60} values in Fig. 1 are in agreement with previous BBOA studies (Cubison et al., 2011; Jolleys et al., 2015; Adler et al., 2011) which are typically situated within the triangular bounds of f_{44} (0.05-0.25) vs f_{60} (0.01-0.04) observed by Cubison et al. (2011). Overall, these results indicate the oxidation of POA from fresh domestic BB emissions to form oxidised POA (oPOA) and SOA which are indistinguishable with respect to f_{44} and f_{60} (Budisulistiorini et al., 2021). Multiple aging processes such as the evaporation of semi-volatile species, condensation of oxidised vapours and the photochemical formation of SOA could contribute to the increased f_{44} in the aged OA.

The concentration of NO_x was greater from the flaming dominated emissions compared to the smouldering dominated phase as shown in Fig. A2a which is as expected and in agreement with previous flaming phase observations (Andreae and Merlet, 2001; Andreae, 2019; Gilman et al., 2015; Roberts et al., 2020). The ratio of $NO:NO_2$ was used to infer the photochemical conversion of NO to NO_2 (Fig. A2b) indicative of the oxidation of VOCs, which results in the production of secondary species such as O_3 and SOA. $NO:NO_2$ ratios were initially higher under the flaming dominated conditions compared to smouldering dominated emissions which is consistent with NO as the end product of nitrogen oxidation at higher temperatures (Lobert and Warnatz, 1993) and flaming as a more efficient burn phase. In the smouldering phase, NO_2 emission can account for up to 40%
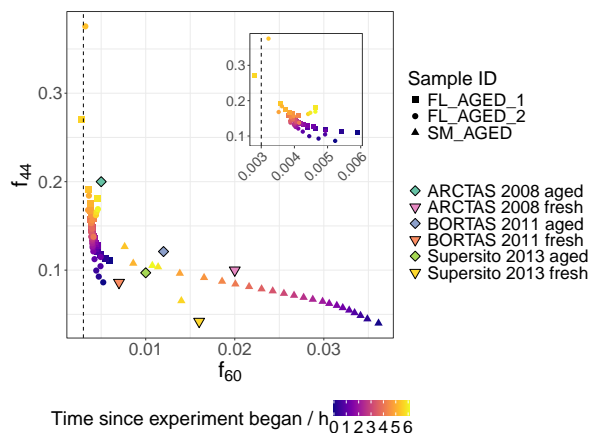
Figure 1. Online AMS measurements of f_{44} and f_{60} for flaming dominated (circle and square points) and smouldering dominated (triangle points) burn phase during the aging experiments, averaged to 15 minute intervals. Sample IDs are given by the point shape. The inset plot displays the zoomed in flaming data. The colour of the points represents the time since the experiment began. The vertical dashed line at $f_{60} \approx 0.3\%$ represents non biomass burning influenced OA ((Cubison et al., 2011)). Aircraft campaign (ARCTAS and BORTAS) and long term site measurements from Cubison et al. (2011); Jolleys et al. (2015); Brege et al. (2018) are presented. The measurements took place over North America (ARCTAS), Canada (ARCTAS and BORTAS) and Northern Italy (Supersito).

of the total NO_x (Lobert and Warnatz, 1993) resulting in a lower $NO:NO_2$ ratio which is in agreement with the observed NO_2 contribution (36%) to the total initial NO_x during the smouldering dominated phase in this study. After aging the $NO:NO_2$

275 ratios in both burn phases converge to a steady state (≈ 0.2) in Fig. A2b as NO is photochemically converted to NO_2, through the reaction with peroxy radicals formed from BBVOC oxidation. As observed in Fig. 1 this indicates aged OA will contain a mixture of POA, oxidised POA (oPOA) and SOA. Ambient BB plumes report $NO:NO_2$ ratios up to 3-5 (Jenkins et al., 1991; Oppenheimer et al., 2004) which are greater than those presented in Table 1 suggesting an increased proportion of NO_2 in this work. This was observed in a previous chamber study and attributed to the presence of O_3 within a dark chamber (Delmas et al.,

280 1995). However, due to interference from conjugated VOCs the concentrations of O_3 inside the chamber cannot be accurately quantified from the UV measurements. Overall online measurements show that the burn phase influences the initial conditions inside the chamber including trace gas concentration and OA composition which can lead to differences in the atmospheric aging of OA.

3.2 Non-target analysis of organic aerosol derived from different burn phases

285 The NTA methodology described in Sect. 2.2 enables large quantities of chemical information to be obtained for all detected compounds, including those with unknown structural identities (Evans et al., 2024). Table A1 shows some commonly used aerosol metrics, such as O:C, H:C and average molecular formula, calculated using the NTA methodology which indicated the OA to be predominantly comprised of CHO compounds, on average contributing 90 % to the total detected mass. The

NTA molecular formula assignments were used to investigate the composition of domestic BBOA derived from domestic BB
290   emissions via carbon number, double bond equivalents (DBE) (Eq. 1) and aromaticity index (AI) distributions (Koch and
Dittmar, 2016).

$$DBE = 1 + C - \frac{H}{2} + \frac{N}{2} \qquad (1)$$

$$DBE_{AI} = 1 + C - \frac{O}{2} - S - \frac{H}{2} - \frac{N}{2} \qquad (2)$$

$$C_{AI} = C - \frac{O}{2} - S - N \qquad (3)$$

295
$$AI = \frac{DBE_{AI}}{C_{AI}} \qquad (4)$$

3.2.1 Chemical composition of organic aerosol derived from flaming dominated emissions

In POA from flaming emissions, CHO compounds have two main regions of high abundance between C_8-C_{11} and between
C_{13}-C_{17} as shown in Fig. 2a. In the first region the DBE ranges between 4-7 (Fig. 2a) which is indicative of aromatic species
which typically possess a DBE of 4 or more. The presence of DBE values greater than 4 coupled with >C_6 suggests these
300   CHO species could be functionalised monoaromatics or small oxygenated polyaromatic species, for instance, napthalene-like
species (C_{10}) which comprise two fused aromatic rings. Using the aromaticity index (Koch and Dittmar, 2016) (Eq.2-4) to
classify species as non-aromatic, monoaromatic or polyaromatic, 51 % and 6% of the detected CHO mass was monoaromatic
and polyaromatic respectively. Between C_8-C_{11} the AI suggests approximately 42% of the mass in this region as monoaromatic
in nature (Fig.A3a). This coupled with > C_6 strongly indicates the presence of functionalised monoaromatics in the first region,
305   such as, phenoxyacetic acid ($C_8H_8O_3$) and phenyl acetic acid ($C_8H_8O_2$) which were identified using authentic standards. In
the second region of high abundance between C_{13}-C_{17} the DBE has a larger range of 6-12 (Fig. 2a). From Fig. 2a and Fig.
A3a, the second region at C_{13}-C_{17} contains DBE values which are generally double that of the first region and the AI suggests
that the mass in this region is predominantly monoaromatic in nature (65 %). This suggests these compounds contain two
aromatic rings linked via short sections of C-H and C=O bonds reflecting the structure of lignin. Figure A3a also shows a small
310   contribution of polyaromatic compounds in the C_{13}-C_{17} region, with a relative contribution of 10 % on average. This is in
accordance with observations of PAH emissions in previous studies from flaming combustion (Sekimoto et al., 2018; Stefenelli
et al., 2019; Bertrand et al., 2018), however, it is clear for this study monoaromatics are of greater quantity in fresh emissions.
In a NTA of ambient BBOA, Brege et al. (2018) observed a peak in relative abundance of CHO species at C_{15} - C_{16} which was
attributed to terpene SOA products. However, in Fig. 2a there is no evidence of sesquiterpene ($C_{15}H_{24}$) derived SOA products
315   which would have relatively low DBE values. Liang et al. (2022) previously observed chamber studies often underrepresent
BB terpene sources due to the lack of distillation from nearby heated and unburnt vegetation. Given that domestic BBOA is the
combustion of non-living material, terpene derived SOA products could be more important in ambient BBOA from wildfires
or crop burning in the presence of live vegetation.
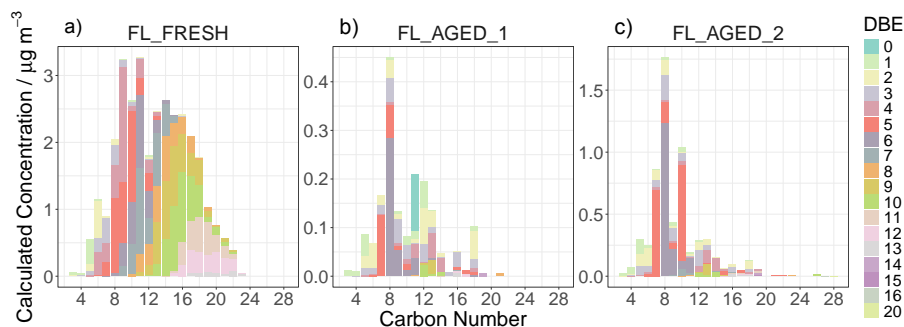
Figure 2. Carbon number vs concentration distribution coloured by the Double Bond Equivalent (DBE) of CHO compounds present in the POA from fresh emissions from flaming dominated burning conditions and after aging (POA+oPOA+SOA). The different filter sample IDs from the flaming dominated combustion experiments are given in each panel a) fresh b-c) aged

After photo-oxidation inside the chamber, the CHO carbon distribution is shifted to lower carbon number species (C_7-C_{10}) in Fig. 2b-c indicating the fragmentation of the larger species with aging. At the same time the main peak in the oxygen distribution increases from $C_xH_yO_2$ to $C_xH_yO_4$ indicating more oxidised CHO compounds in the aged aerosol (Fig. A4a-b). Li et al. (2021) suggested the higher NO_x concentrations from flaming emissions could promote fragmentation pathways through the reactions of peroxy radicals (RO_2 + HO_2) with NO. However, other processes such as photolysis and heterogeneous photo-oxidation may also result in the production of small molecules. The aged C_7-C_{10} CHO compounds possess DBEs in the range of 2-6 indicating some formation of non-aromatic compounds. However, using the AI, after atmospheric aging the CHO composition of the OA from flaming dominated emissions still contained a large degree of aromatic character (41%). The largest peak in the aged distributions in Fig. 2b-c at C_8 has a DBE value of 6 and is predominantly monoaromatic in nature (Fig. A3b). The mass of this peak is dominated by $C_8H_6O_4$ which can be attributed to phthalic acid from previous observations (Wang et al., 2017a; Qi et al., 2019) and $C_8H_8O_3$ was confirmed as vanillin using an authentic standard.

For the CHON species, POA from flaming emissions has a main peak in the carbon number distribution at C_6 (Fig. A5a) and approximately 74 % of the detected CHON mass in fresh OA has an O:N ratio $\geq$ 3 suggesting the presence of a nitro (-NO_2) group. Using a modified AI calculation derived for this work to account for the presence of the two N-O bonds within a -NO_2 group (Eq 5-7), 42% of the detected CHON mass is aromatic in nature. As shown in Fig. A5a the aromatic mass is predominantly comprised of C_6 monoaromatic compounds which coupled with the large proportion of nitro containing compounds is highly indicative of nitro-monoaromatic species. For instance, 3-nitrophenol ($C_6H_5NO_3$) and 4-nitrocatechol ($C_6H_5NO_4$) were detected in the fresh OA and have been commonly observed as tracers of BB in previous studies (Claeys et al., 2012; Kourtchev et al., 2016; Iinuma et al., 2010; Kitanovski et al., 2012; Budisulistiorini et al., 2017; Li et al., 2017). After photo-oxidation the relative ratio of CHO:CHON concentration decreases from 41.5 to 8.7-9.2 (Table A1) indicating an increased contribution of CHON compounds to the aged OA composition. In the aged OA, the abundance of larger compounds

340 (ie. > C_{10}) increases, in particular polyaromatic C_{12}-C_{14} species, such as $C_{12}H_9NO_4$ which accounts for 10% of the total CHON aromatic mass (Fig. A5b). Zhang et al. (2013) previously observed $C_{12}H_9NO_4$ in ambient OA from the Los Angeles basin which had significant contributions from anthropogenic emissions and wood burning sources, however it was attributed to a nitro-monoaromatic compound. Whereas, in this work we assign $C_{12}H_9NO_4$ as a derivative of napthalene using the modified AI in Eq 5-7. Furthermore, the percentage mass of CHON with an O:N ratio $\geq$ 3 remained largely unchanged ($\approx$ 70 %) after

345 aging indicating CHON in aged OA are also predominantly NACs. Overall, the aged OA CHON composition contains a similar contribution of NACs to the POA which could be a result of the combination of unreacted species, loss of oxidation products to the gas phase and the condensation of new secondary products to the particle phase.

$$DBE_{\text{CHON}} = 1 + C - \frac{O-2}{2} - S - \frac{H}{2} - \frac{N-1}{2} \tag{5}$$

$$C_{\text{CHON}} = C - \frac{O-2}{2} - S - (N-1) \tag{6}$$

350
$$AI_{\text{CHON}} = \frac{DBE_{\text{CHON}}}{C_{\text{CHON}}} \tag{7}$$

3.2.2 Chemical composition of organic aerosol derived from smouldering dominated emissions

The measured carbon distribution of POA from a fresh smouldering dominated burn shows a peak between C_8-C_{11} (Fig. 3a) which largely has DBEs in the range of 4-8 and the AI estimated the majority of the mass in this carbon number region as aromatic (54.4%). The largest peak in the distribution shown in Fig. 3a is from C_{10} compounds with a DBE of 6 predominantly

355 consisting of $C_{10}H_{10}O_3$ which was previously attributed to coniferylaldehyde in BBOA (Fleming et al., 2020; Smith et al., 2020). Furthermore, Figure A3c shows the majority of the CHO compounds are aromatic with a 50% and 16% contribution from monoaromatic and polyaromatic species respectively. This indicates the C_8- C_{11} species are predominantly functionalised monoaromatic compounds as similarly observed for flaming. However, in this region there is also a greater concentration of polyaromatic compounds compared to flaming OA (see Figure A3), such as $C_{11}H_8O_2$ and $C_{11}H_8O_3$ which are naphthoic acid

360 derivatives previously observed in primary and secondary wood combustion products (Bruns et al., 2015). From Figure A3 the smouldering dominant POA shows an increased concentration of smaller C_{11}-C_{12} oxygenated PAHs (o-PAHs) compared to flaming dominant POA which has the largest contribution from C_{14} o-PAHs. A previous study observed the formation of PAHs and o-PAHs was dependent on the temperature and oxygen availability observing at higher temperatures in the absence of oxygen larger PAHs can form whilst smaller PAHs arise at lower temperatures (Fitzpatrick et al., 2008). Therefore the

365 relative PAH concentration and PAH composition will be dependent on the burn phase. Furthermore, the observed increased contribution of o-PAHs in the smouldering dominated burn is in agreement to findings by Orasche et al. (2013). In addition to functionalised monoaromatic compounds contributing to the C_8-C_{11} peak, such as, phenylacetic acid ($C_8H_8O_2$) and 3-(4-hydroxyphenyl)propionic acid ($C_9H_{10}O_3$), a previous study found smouldering had higher emissions of methoxyphenols (Kjällstrand and Olsson, 2004) which possess > C_7 and is consistent with the observed range of carbon numbers and DBE

370 values in Fig. 3a.
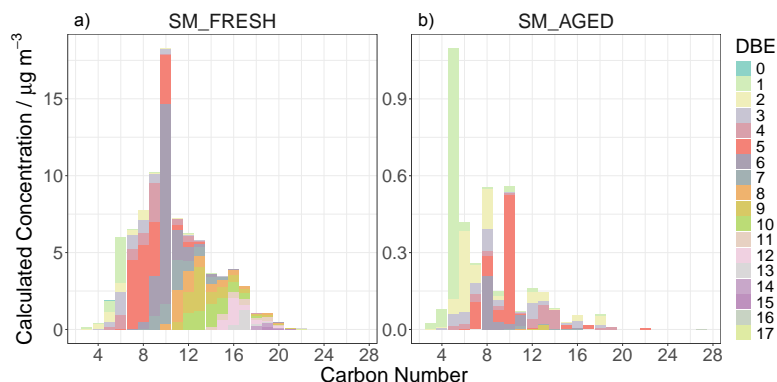
Figure 3. Carbon number vs concentration distribution coloured by the Double Bond Equivalent (DBE) of CHO compounds present in the POA from fresh emissions from smouldering dominated burning conditions and after aging (POA+oPOA+SOA). The different filter sample IDs from the smouldering dominated combustion experiments are given in each panel a) fresh b) aged

After photo-oxidation, the main region in the carbon number distribution reduces to C_5-C_8 (Fig. 3b) with a second prominent peak at C_{10}. The DBE range also decreases to 1-6 after aging. The AI values indicate a large reduction in aromaticity after atmospheric aging as the percentage contribution of aromatic CHO to the detected mass decreases from 66% to 13%. Brege et al. (2018) observed a comparable shift to lower DBEs (1-5) in ambient BBOA after aging and Fang et al. (2021) showed SOA from oxidised smouldering POA had significant contributions from oxygenated aliphatic species. From the oxygen number distribution shown in Fig. A4c-d the main peak increases from $C_xH_yO_3$ to $C_xH_yO_4$ indicating the presence of more oxidised species in aged OA. Overall, this suggests OH functionalisation products contribute to the aged OA as well as the significant fragmentation of aromatic ring containing species from the POA. In Fig. 3b, the peaks between C_4-C_6 with DBEs of 1-2 are largely comprised of small but highly oxidised species such as $C_4H_8O_4$, $C_5H_{10}O_4$, $C_5H_8O_{3-5}$ and $C_6H_{10}O_{4-5}$. Kalogridis et al. (2018) observed higher emission factors of succinic and glutaric acids in smouldering compared to flaming therefore, these species could be derivatives of succinic acid (C_4) or glutaric acid (C_5) (Kalogridis et al., 2018; Kundu et al., 2010; Liang et al., 2021). This could also explain the lack of low DBE C_4 and C_5 compounds in the carbon number distribution derived from flaming dominated OA shown in Fig. 2b-c. $C_5H_{10}O_4$ was also previously attributed to deoxyribose in BBOA (Smith et al., 2020), however this is likely not detected by the negative mode UHPLC-HRMS. The remaining aromatic mass after photo-oxidation in smouldering dominated OA is predominantly formed of C_7-C_8 monoaromatic species (Fig. A3d), such as, vanillin in addition to $C_8H_6O_4$ and $C_7H_6O_2$ which were previously attributed to phthalic acid and benzoic acid respectively (Wang et al., 2017a). Phthalic acid and benzoic acid were also identified as oxidation products of napthalene (Wang et al., 2017a) which is in agreement with the observed reduction in polyaromatic C_{10}-C_{11} species in Fig. A3. Similar to flaming, polyaromatic species contributions were significantly reduced after aging in agreement with previous studies, which observed the emission factors of o-PAHs to decrease by 20 % between fresh and aged BBOA (Li et al., 2020) and the degradation of

particle bound PAHs after aging smoke particles (Kim et al., 2023b). Considering the damaging health impacts of oxygenated PAHs, the reduction of their contribution with aging could lead to important implications for the OA toxicity.

For CHON species, the fresh OA distribution shows high concentrations at C_9 for non-aromatic compounds and C_6 for monoaromatic species (Fig. A5c) which is similar to the peak in C_6-C_{10} CHON species observed in ambient fresh BBOA (Brege et al., 2018). These peaks predominantly consist of species such as $C_9H_{11}NO_4$ and $C_6H_5NO_5$ which were previously observed in ambient cloud water samples influenced by agricultural BB (Desyaterik et al., 2013) and in fresh BBOA from controlled burn experiments (Lin et al., 2016). In addition, 72% of the CHON mass had a O:N $\geq$ 3 suggesting the presence of -NO_2 functionality. This is therefore in accordance with Lin et al. (2017) who attributed $C_6H_5NO_5$ in BrC originating from a major BB event to nitrobenzenetriol. After photooxidation inside the chamber the CHO:CHON concentration ratio decreases from 29.2 to 10.9 (Table A1) indicating a greater contribution of CHON species to the overall OA composition. Similar to flaming, the OA distribution in Fig. A5d shows an increase in larger CHON species (ie. > C_{10}) after aging. Monoaromatic compounds in the aged OA, are predominantly comprised of C_5, C_6 and C_{12} species such as $C_5H_5NO_4$, $C_6H_5NO_3$, $C_6H_4N_2O_5$ and $C_{12}H_{12}N_2O_4$ (Fig. A5d). $C_6H_5NO_3$ and $C_6H_4N_2O_5$ were identified as 3-nitrophenol and 2,4-dinitrophenol respectively using authentic standards and $C_5H_5NO_4$ was previously observed in BrC from a major BB event (Lin et al., 2017) but the structure could not be elucidated. However, a monoaromatic C_5 species is indicative of furanic origins as previous observations indicate furans are important for SOA production in smouldering fires (Stefenelli et al., 2019). In the aged OA, the relative contribution of aromatic compounds to the CHON mass decreased from 45% to 31 % and the proportion of compounds with O:N $\geq$ 3 reduced to 47% which overall indicates a reduction in the contribution of NACs to the OA composition after atmospheric aging.

3.3 Impact of the burn phase on the oxidation and aged chemical composition of organic aerosol

As discussed in Sect. 3.2.1 and 3.2.2 the burning conditions influence the POA composition and POA mass with subsequent atmospheric aging producing two unique distributions (see Fig. 2 and Fig. 3), which could enable the development of burn-specific tracer species. However, overall there is a comparable contribution of aromatic species (> 50%) to the POA composition under both conditions which is in accordance with Akherati et al. (2020) and Gilman et al. (2015) who observed oxygenated aromatics had the greatest SOA formation potentials and contributed to nearly 60 % of the SOA mass from BB. However after aging, the change in the contribution of aromatic compounds to the OA composition differed with a significant reduction observed for smouldering dominated compared to flaming dominated burns. In particular, smouldering dominated emissions showed a greater reduction in polyaromatic contributions to the OA mass after aging (-16.2%) compared to the flaming dominated phase (-2.6%). This difference in compositional change indicates aging of OA from smouldering emissions could result in more oxidised products compared to flaming.

In order to compare the effect of atmospheric aging processes on the OA composition from domestic BB, O:C ratios of aromatic and non-aromatic compounds were examined via their probability density distributions which visualise the differences in the population of observable O:C values. The distribution shown in Fig. 4 is constructed using a kernel density estimation which fits a smooth distribution across a series of band widths to a histogram of the observed O:C values in the domestic

425 BBOA samples. The *y axis* represents density meaning the probability of the OA having a certain O:C value can be computed by integrating the area under the curve. In this analysis the peaks in the O:C distributions of fresh and aged OA are examined to observe differences in the composition and hence provide insight into the magnitude of OA oxidation under different burning conditions. Generally, the peak of the O:C distributions in Fig. 4 of aromatic compounds for flaming dominated and smoul­dering dominated experiments show a greater change upon aging compared to non-aromatic species. This demonstrates that
430 oxidation of aromatic compounds is significant for the observed compositional change as inferred from Sect. 3.2.1 and 3.2.2.
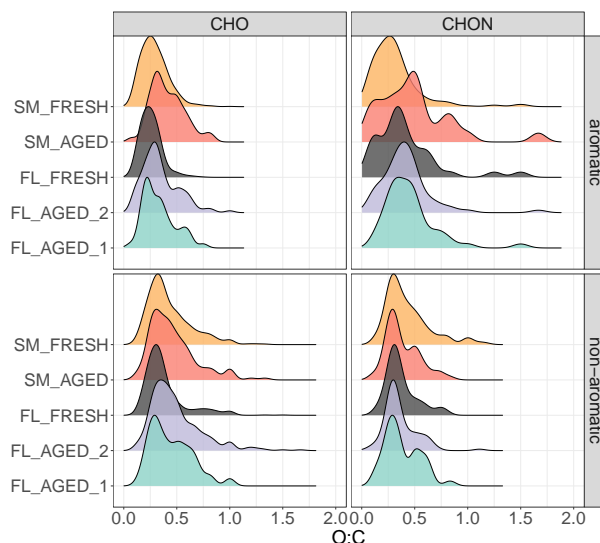
Figure 4. Probability density distribution of O:C ratios of the detected aromatic (top panel) and non-aromatic (bottom panel) CHO (left panel) and CHON (right panel) compounds. The *y axis* height represents density and the area under the curve represents probability. Sample IDs for each burn experiment are given on the *y axis* and the distribution colour.

In the POA from fresh emissions, the average O:C for CHO compounds is generally higher for the smouldering dominated phase than the flaming dominated phase (Table A1). The smouldering dominated POA shows a broader distribution in in Fig. 4 indicating the presence of more oxygenated compounds than from the flaming dominated burns, as seen in the oxygen number distribution (Fig. A4). After aging, the distributions shift to higher O:C values consistent with the observed increased oxygen
435 content and fragmentation of the carbon backbone indicative of the oxidation of OA (Jimenez et al., 2009). For aromatic CHO compounds the increase in O:C after aging is greater in the smouldering dominated burn compared to the flaming dominated burns. In smouldering dominated OA the main peak in the O:C ratio for aromatic CHO compounds increased from 0.25 to 0.50 with a smaller peak at 0.80. Upon aging in the flaming dominated burn the main peak of the O:C ratio increased from 0.22 to 0.29 with a smaller peak at 0.50. Furthermore, the area under the distribution represents probability and at the O:C value of
440 0.50, the area was greater for smouldering dominated than flaming dominated phases suggesting a larger number of oxidised

species. Additionally the presence of high O:C values (≈ 0.80) from the smouldering dominated phase derived OA which are absent in the flaming dominated burn distribution similarly indicates a greater proportion of increasingly oxidised compounds. This is in agreement with Li et al. (2021) who observed greater oxidation of smouldering emissions compared to flaming.

For aromatic CHON species, there is a significant difference in the POA probability density distributions with a broader distribution in the smouldering dominated phase compared to 3 resolved peaks for the flaming dominated phase. The smouldering dominated POA distribution peaks at an O:C value of 0.25 whereas the flaming dominated POA distribution contains 3 distinct peaks at O:C ratios of 0.15, 0.34 and 0.60 with the greatest density at 0.34. However, the lower value of the O:C ratio peak in smouldering dominated POA compared to flaming dominated POA could be due to the greater contribution of polyaromatic species (Fig. A3) which typically possess relatively low O:C values. Similarly, after aging the O:C distributions in Fig. 4 show different trends for flaming dominated and smouldering dominated experiments. In smouldering dominated aged OA there is a clear increase in O:C from 0.25 to 0.47 which is in agreement with previous observations of the change in O:C (0.09-0.30) from smouldering fires (Bertrand et al., 2017; Grieshop et al., 2009; Tasoglou et al., 2017). Whereas for flaming, the distributions of aromatic CHON compounds are relatively similar between fresh and aged OA and the increase in O:C from the main peak is relatively low (0.07). $C_6H_5NO_3$ (nitrophenol), $C_7H_7NO_4$ (nitroguaiacol) and $C_{10}H_7NO_3$ (nitro-1-napthol) were identified in both POA and aged OA from the flaming dominated phase with an increase in concentration after aging, indicating the formation of similar CHON compounds to POA during photo-oxidation.

Overall, the observed values of O:C in CHO compounds for both flaming and smouldering in Fig. 4 are in a similar range to O:C reported in ambient BBOA (0.42 - 0.47) (Dzepina et al., 2015; Brege et al., 2018). Furthermore, CHON species from ambient OA influenced by varying degrees of BB were reported to have O:C values in the range of 0.37-0.50 (Lin et al., 2012; Kourtchev et al., 2016; An et al., 2019; Dzepina et al., 2015) which is similar to the peak O:C range shown in Fig. 4. However, the O:C values reported in these studies include both aromatic and non-aromatic species and are weighted by relative abundance derived from limited metrics, such as, peak area or the number of detected formulas.

Van Krevelen diagrams of the O:C vs H:C space can also provide insight into the differences in composition and atmospheric aging between smouldering and flaming derived OA (Fig. 5). For instance, POA derived from fresh smouldering dominated emissions had a greater range of O:C values across a similar range of H:C ratios as fresh flaming dominated emissions in Fig. 5 suggesting increasingly oxygenated OA. In addition, Fig. 5 shows POA from fresh smouldering dominated emissions has a greater quantity of polyaromatic CHO and CHON compounds as previously observed in Fig. A3 and Fig. A5. After aging, there is a significant reduction in aromatic species for the smouldering dominated phase and to a lesser extent in the flaming dominated phase (Fig. 5). In the aged OA from smouldering dominated emissions the reduction in polyaromatic compounds is significantly greater compared to flaming dominated derived OA, with almost complete loss of the polyaromatic CHO species in Fig. 5. Whereas for flaming dominated OA, the number of aromatic CHON species in the Van Krevelen space increased after aging, notably for polyaromatic CHON species. This trend can also be seen for the flaming experiments in Fig. A5 with increased C_{12}-C_{14} polyaromatic CHON species in aged OA and a simultaneous decrease of C_{12}-C_{14} polyaromatic CHO species in Fig. A3. Therefore, this suggests the formation of NACs from the oxidation of aromatic CHO compounds during the flaming dominated phase. The same trend was also observed in the Van Krevelen of species detected in positive mode ESI (Fig. A6).

The production of NACs could be greater from the flaming dominated burn since NO_x emissions from flaming are typically higher than smouldering (Fig. A1a) thus leading to the formation of ring retained nitroaromatic species.
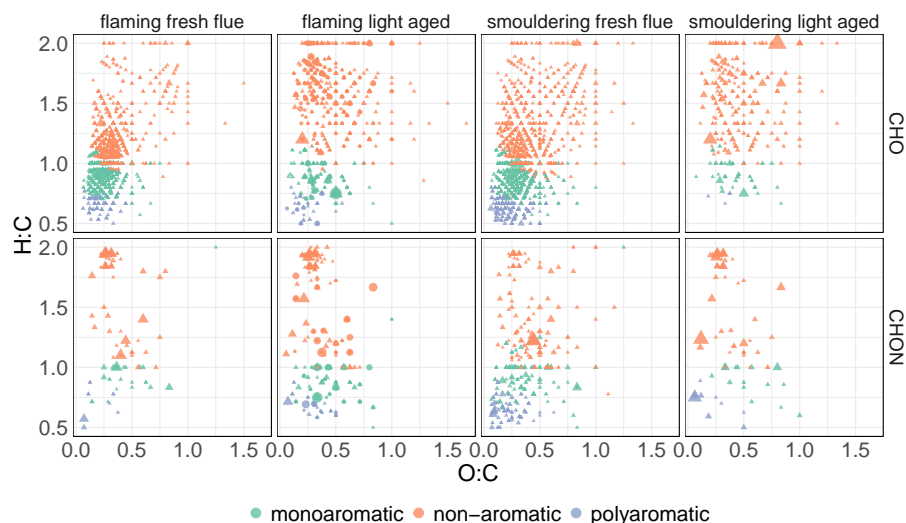
Figure 5. Van Krevelen diagrams of H:C vs O:C ratios for CHO (top row) and CHON (bottom row) compounds derived from flaming dominated and smouldering dominated burn phases, coloured by the aromaticity index assignment (non-aromatic: AI < 0.5, monoaromatic: $0.5 \leq AI \leq 0.67$, polyaromatic: AI > 0.67). In the flaming light aged panel the point shape represents the two repeats: FL_AGED_1 (circles) and FL_AGED_2 (triangles)

The notable variation of the aromatic contribution to aged OA compositions and significant differences in the concentration of polyaromatic species between burn phase could thereby have important implications for toxicity. Kim et al. (2023b) previously investigated the toxicity of wood smoke particles and observed that after aging the mutagenicity was lower compared to fresh particles when considering PAHs. Furthermore, on an equal particle mass basis aged flaming smoke particles had a higher potential toxicity value with respect to PAHs than aged smouldering smoke particles (Kim et al., 2023b). This could potentially be the result of an increased fraction of nitro-PAH compounds from flaming (Fig. 5), some of which are known to exceed the toxicity of their parent PAH. Therefore, the OA composition under different burning conditions can be an important factor affecting the toxicity but often the greater observed emission factors from smouldering (Zhang et al., 2022; Jen et al., 2019) prevail in the determination of the toxicity.

The volatility of the domestic BBOA was estimated using the 2-dimenstional volatility basis set (2D-VBS) parameterisation described in Li et al. (2016) (see Appendix A1) to determine differences in aging processes which could explain the observed differences in composition. The 2D-VBS estimation error was shown to increase for lower saturation mass coefficients therefore

490 some caution must be taken when considering low volatility products (Li et al., 2016). Figure A7 shows the Van Krevelen distribution coloured by the OA volatility which indicates after aging there is a slight increase in volatility likely from the formation of smaller compounds as shown in Sect. 3.2.1 and 3.2.2. For the smouldering dominated burn aging resulted in the almost complete loss of low volatile organic compounds (LVOC) and semi-volatile organic compounds (SVOC) from the POA. OA from the flaming dominated phase in the region of H:C < 1 and O:C < 0.5 conversely showed a notable increase in the

495 SVOC CHON compounds and a simultaneous reduction of SVOC CHO compounds, suggesting the formation of NACs after aging as observed in Fig. 5. This difference in processing between the burning conditions is in accordance with Kalogridis et al. (2018) who similarly observed changes in OC from flaming to be driven by the production or partitioning of organic compounds to the particle phase whereas for smouldering, evaporation of semi-volatile species was considered an important sink of OC.

500 Generally, the observed O:C ratios of the aromatic compounds in aged OA shown in Fig. 5 are in agreement with those for SOA derived from aromatic oxidation (eg. toluene, m-xylene and napthalene) with reported values ranging between 0.57-0.75 (Chen et al., 2021, 2020; Loza et al., 2012; Chhabra et al., 2010) and the observed range for phenolic SOA oxidation products (0.3-1.0) (Ofner et al., 2011). Furthermore, the observable H:C vs O:C space in Fig. 5 is within the range reported for lignin-like compounds (1-1.5 vs 0.2-0.6) (An et al., 2019) as expected for BBOA. Overall, these results show SOA from

505 aromatic compounds via ring-opening and ring retained nitroaromatic formation routes contribute substantially to the aged OA composition and may have important implications for atmospheric chemistry (Bloss et al., 2005).

4   Conclusions

The chemical composition of domestic biomass burning organic aerosol (BBOA), from a series of controlled burn chamber experiments, was investigated using a newly developed semi-quantitative non-target analysis (NTA) methodology and is the

510 first study to account for ionisation effects in an NTA of BBOA using retention window scaling (Evans et al., 2024). The NTA approach enabled the detection of up to 2357 features in a single sample (Evans et al., 2024) which is simply impossible from a targeted approach with a limited number of standards. Significant compositional differences between the organic aerosol (OA) derived from emission under different burn phases (i.e. flaming dominated and smouldering dominated phases) and after aging were observed. However, the experimental methodology used here could be improved by sampling directly from the chamber

515 at the start of the experiment but this remains challenging for offline approaches due to the higher sample volume required and the low particle mass used in this study. Overall, the composition of domestic BBOA was dominated by oxygenated compounds (CHO). On average CHO compounds constituted 90% of the total detected mass with a smaller contribution ($\leq$ 10%) of organonitrogen species (CHON), which suggests the wide usage of nitroaromatic compounds as tracers of biomass burning may not be ideal as these compounds typically have high ionisation efficiencies and therefore appear more abundant

520 when using peak area metrics. In agreement with other studies, the estimated concentrations of the detected compounds were markedly higher in OA from smouldering dominated emissions compared to flaming dominated emissions, as a result of the larger OA emission factors associated with smouldering. This indicates the burn phase in a domestic environment is a critical

factor for controlling indoor air pollutant concentrations along with air filtration and the stove model (Ward et al., 2015). Considering the OA chemical composition from fresh emissions, flaming dominated POA had a large contribution of CHO compounds between C_8-C_{11} and C_{13}-C_{17} which were predominantly comprised of functionalised monoaromatic compounds. Smouldering dominated POA emissions had a higher concentration of lower molecular weight CHO species, predominantly in the region of C_8-C_{11} with a peak at C_{10}, which were also attributed to functionalised monoaromatic compounds. Furthermore, smouldering dominated POA also had a greater percentage contribution from o-PAHs of 16% over the same carbon range compared to the flaming dominated POA (6%) which has important implications for the toxicity of POA. For CHON species, the observed POA composition contained comparable concentrations of C_6 monoaromatic species between the burn phases that were largely assigned as NACs such as widely used BB tracers, nitrophenols and nitrocatechols. However, after aging, the OA composition between the burning conditions significantly diverged particularly in the relation to the contribution of aromatic CHO and CHON compounds to the aged OA composition which was attributed to burn specific aging processes. For OA from the smouldering dominated phase, aging decreased the relative contribution of aromatics with almost complete reduction of both polyaromatic CHO and CHON species resulting in the formation of ring-opened products. In comparison, for the flaming dominated burns, the reduction in the contribution of aromatic compounds to the detected OA mass after aging was less than in smouldering and Van Krevelen analysis indicated the number of polyaromatic CHON species notably increased, suggesting the formation of NACs from aromatic CHO species. These differences in the aromatic contribution to the OA composition between the burn phases have important implications for toxicity, particularly in relation to polyaromatic species which are known carcinogenic species. The formation of ring retained NACs from the flaming dominated burns highlight important implications for both toxicity and BrC formation. In contrast, higher volatility ring-opened products were an important contribution to OA from aged smouldering dominated emissions. These products could volatilise from the particulate phase and impact on atmospheric chemistry and O_3 formation, invariably leading to the creation of compounds of unknown toxicities. At present, toxicology endpoints used for policy-making decisions on mitigating impacts for human health are typically based on mass. In reality, this is a more complex picture with multiple factors affecting the toxicity of domestic BBOA such as the emission factor of a compound, the OA composition as studied here, the total mass of fuel burnt and ultimately the length of time exposed to the emission.

Author contributions. RLE prepared the manuscript with contributions from co-authors. The wood burning experiments were predominantly designed by AV and GM with input from all authors. Chamber experiments were performed by AV, DH, HW, SAS, OEO and RLE. SAS and HW provided trace gas and AMS measurements from the Manchester Aerosol Chamber. Offline filter sample measurements and non-target analysis was conducted by RLE. DJB contributed to scientific discussion. JFH and ARR supervised the project and obtained funding to develop the methodology.

Competing interests. The authors declare no competing interests

Acknowledgements. The Manchester Aerosol Chamber receives funding from the Horizon 2020-Research and Innovation Framework Programme, H2020-INFRAIA-2020-1, Sustainable Access to Atmospheric Research Facilities (ATMO-ACCESS), Grant Agreement number: 101008004. The Orbitrap MS at the University of York was funded by a Natural Environment Research Council (NERC) strategic capital grant (grant no. CC090). The authors thank the NERC Panorama Doctoral Training Partnership (DTP), under grant NE/S007458/1 for the studentship of Rhianna Evans. Sara Syafira acknowledges studentship support from the Indonesia Endowment for Education (LPDP) and Osayomwanbor Oghama acknowledges studentship support from the Tertiary Education Trust Fund (TETFund), Nigeria. Daniel Bryant acknowledges financial support from NERC under grant NE/W002051/1 and NE/S010467/1.

Appendix A
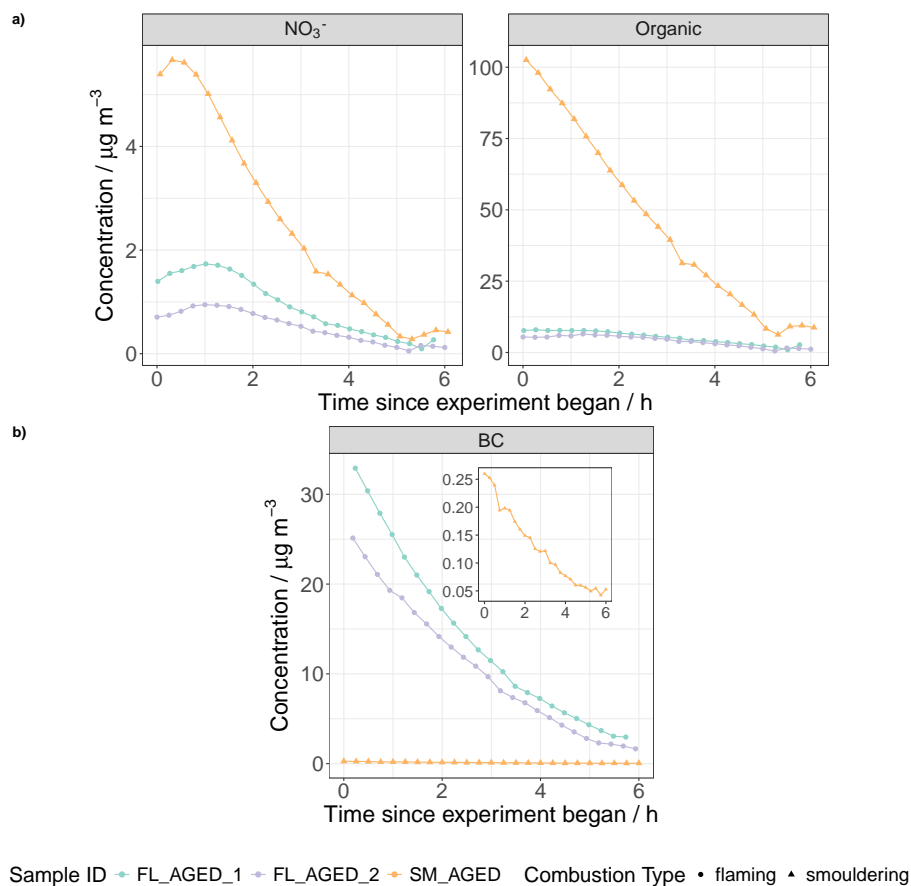
Figure A1. a) Online AMS measurements of NO_3^- and organic fraction concentrations for flaming dominated (circle points) and smouldering dominated (triangle points) aging experiments, averaged to 15 minute intervals, b) BC timeseries averaged to 5 minutes, with sample IDs given by the point or line colour, the inset plot depicts the timeseries from smouldering zoomed in on the *y-axis*.
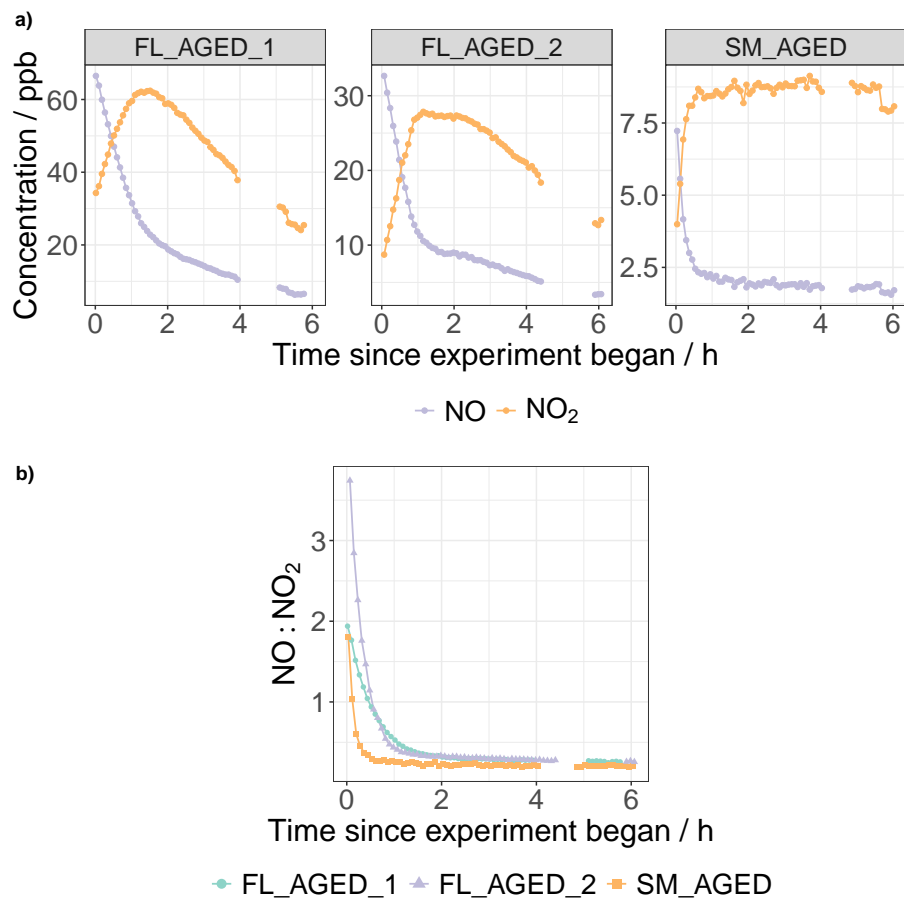
Figure A2. a) NO and NO$_2$ timeseries of the flaming dominated and smouldering dominated aging experiments with individual experiments shown in each panel. b) Ratio of NO:NO$_2$ during the flaming dominated and smouldering dominated aging experiments with the experiment indicated by the line colour. In panel a) and b) data is removed during filter sampling due to interference with the NO$_x$ instrument inlet.

Table A1. Average aerosol metrics calculated from the semi-quantitative NTA methodology of the detected CHO and CHON compounds in the domestic BBOA samples

Sample ID	Category	O:C	H:C	Molecular formula	Relative abundance / %	DBE
FL_FRESH	CHO	0.28	1.05	$C_{12.8}H_{13.0}O_{3.3}$	97.2	7.32
FL_AGED_1	CHO	0.42	1.39	$C_{10.1}H_{14.6}O_{3.8}$	84.6	3.82
FL_AGED_2	CHO	0.41	1.19	$C_{9.3}H_{11.3}O_{3.5}$	83.6	4.68
SM_FRESH	CHO	0.35	1.04	$C_{10.6}H_{10.4}O_{3.3}$	96.1	6.41
SM_AGED	CHO	0.54	1.56	$C_{8.0}H_{12.1}O_{3.7}$	84.9	2.95
FL_FRESH	CHON	0.54	1.74	$C_{13.5}H_{23.1}O_{5.2}N_{1.6}$	2.3	3.76
FL_AGED_1	CHON	0.41	1.25	$C_{11.2}H_{14.5}O_{4.3}N_{1.5}$	9.7	5.62
FL_AGED_2	CHON	0.4	1.61	$C_{14.2}H_{23.3}O_{4.6}N_{1.6}$	9.1	4.38
SM_FRESH	CHON	0.42	1.18	$C_{10.4}H_{12.3}O_{3.7}N_{1.3}$	3.3	5.91
SM_AGED	CHON	0.35	1.48	$C_{14.7}H_{21.7}O_{4.1}N_{2.1}$	7.8	5.91
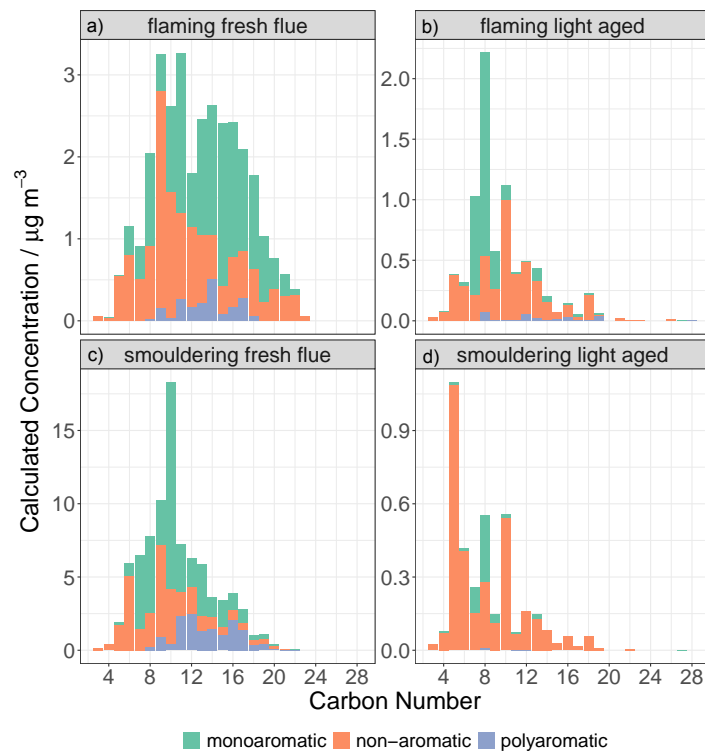
Figure A3. Carbon number distribution of CHO compounds present in the fresh flue emissions (POA) and light aged aerosol (POA+oPOA+SOA) from flaming dominated (a-b) and smouldering dominated (c-d) combustion. The two repeats of the flaming light aged experiment were combined to produce a total concentration in the figure. Coloured by the aromaticity index assignments of non-aromatic (AI < 0.5), mono-aromatic ($0.5 \leq AI \leq 0.67$) and polaromatic (AI > 0.67))
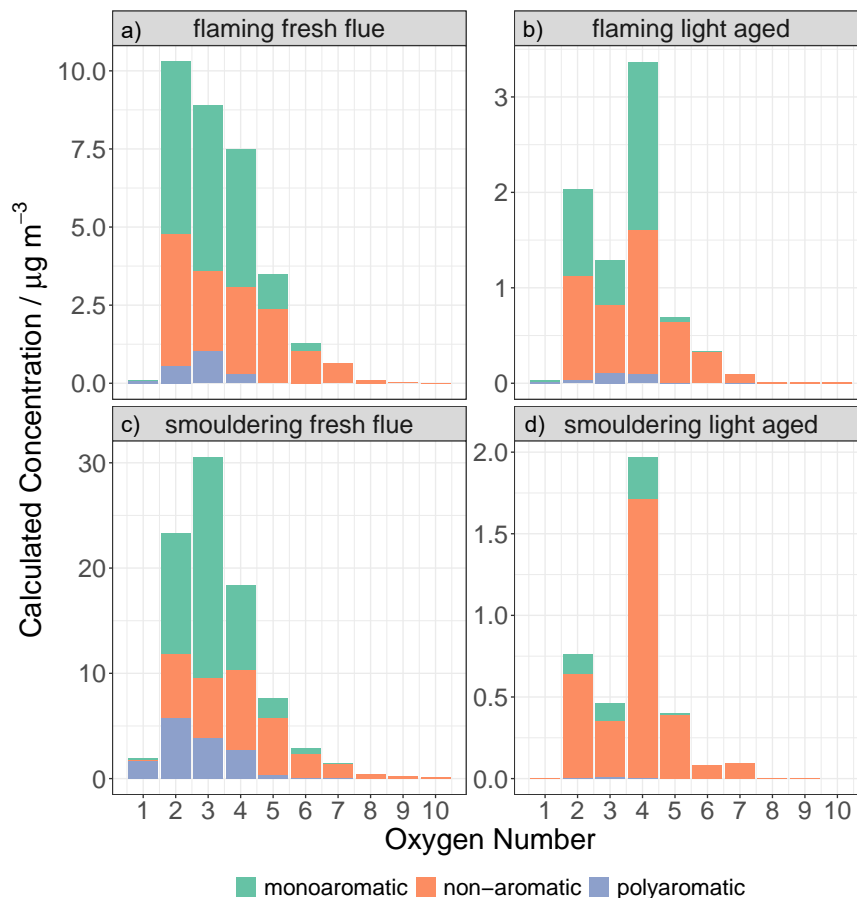
Figure A4. Oxygen number distribution of CHO compounds present in the fresh flue emissions (POA) and light aged aerosol (POA+oPOA+SOA) from flaming dominated (a-b) and smouldering dominated (c-d) combustion. The two repeats of the flaming light aged experiment were combined to produce a total concentration in the figure. Coloured by the aromaticity index assignments of non-aromatic (AI < 0.5), mono-aromatic ($0.5 \leq AI \leq 0.67$) and polaromatic (AI > 0.67)
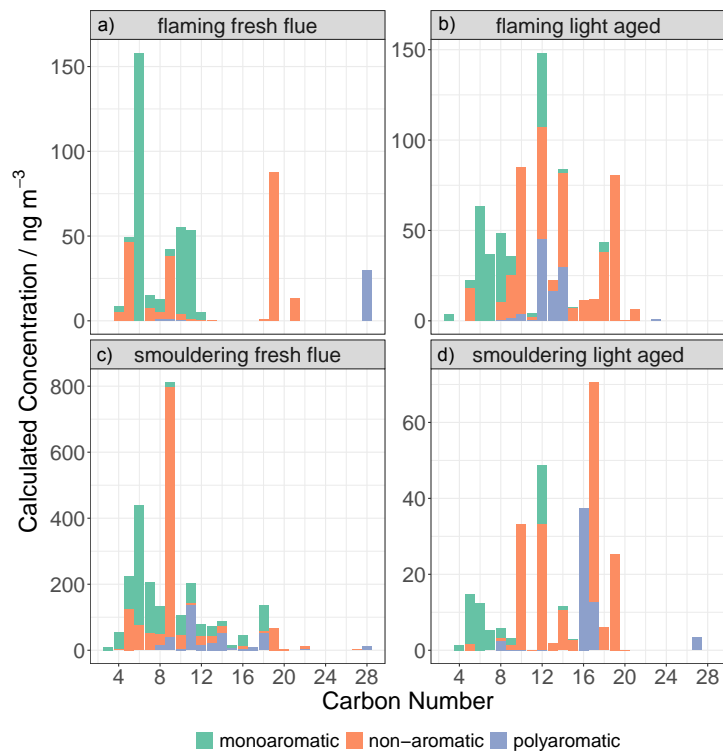
Figure A5. Carbon number distribution of CHON compounds present in the fresh flue emissions (POA) and light aged aerosol (POA+oPOA+SOA) from flaming dominated (a-b) and smouldering dominated (c-d) combustion. The two repeats of the flaming light aged experiment were combined to produce a total concentration in the figure. Coloured by the aromaticity index assignments of non-aromatic (AI < 0.5), mono-aromatic ($0.5 \leq$ AI ≤ 0.67) and polaromatic (AI > 0.67)

Volatility Parameterisation The volatility of the organic aerosol was calculated according to the parameterisation described in Li et al. (2016) using Eq. A1:

$$\log_{10} C_0 = (c^0 - c) \times b_C - n_O \times b_O - 2\frac{n_C \times n_C}{n_C + n_O} \times b_{CO} - n_N \times b_N - n_S \times b_S \tag{A1}$$

565   where c^0 is the reference carbon number, n_C, n_O, n_N, n_S represent the number of carbon or oxygen or nitrogen or sulfur atoms present in the structure, b_C, b_O, b_N, b_S represents the atom contribution to $\log_{10} C_0$ and b_{CO} is the carbon-oxygen non-ideality.

Compounds were classed as volatile organic compounds (VOC) when $C_0 > 3 \times 10^6$ μg m^{-3}, intermediate volatile organic compounds (IVOC) when $300 < C_0 < 3 \times 10^6$ μg m^{-3}, semi-volatile organic compounds (SVOC) when $0.3 < C_0 < 300$ μg m^{-3}, low volatile organic compounds (LVOC) when $3 \times 10^{-4} < C_0 < 0.3$ μg m^{-3} and extremely low volatile organic compounds

570   (ELVOC) when $C_0 < 3 \times 10^{-4}$ μg m^{-3}.
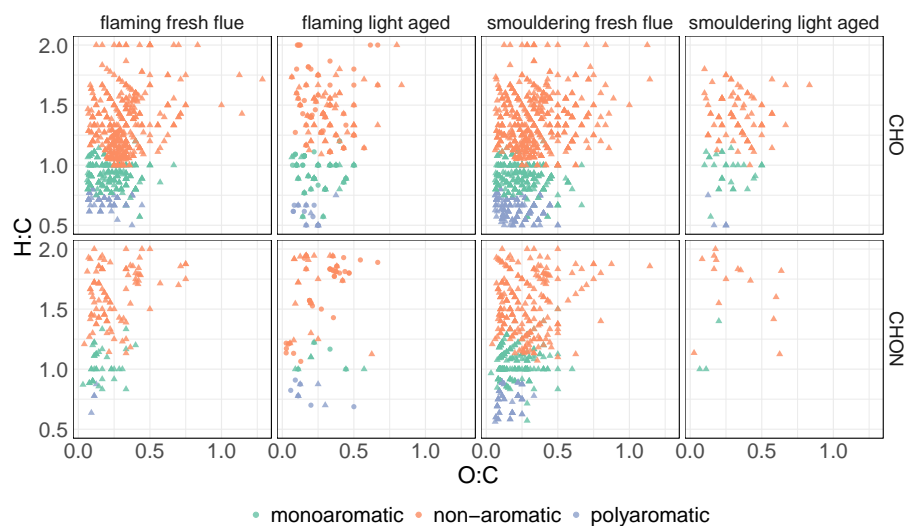
Figure A6. Van Krevelen diagrams of H:C and O:C ratios for CHO (top row) and CHON (bottom row) compounds in OA derived from flaming dominated and smouldering dominated burn phases and detected by positive mode ESI. aromaticity index (AI) assignments are shown by the point colour (non-aromatic: AI < 0.5, monoaromatic: $0.5 \leq AI \leq 0.67$, polyaromatic: AI > 0.67). In the flaming light aged panel the point shape represents the two flaming repeats: FL_AGED_1 (circles) and FL_AGED_2 (triangles)
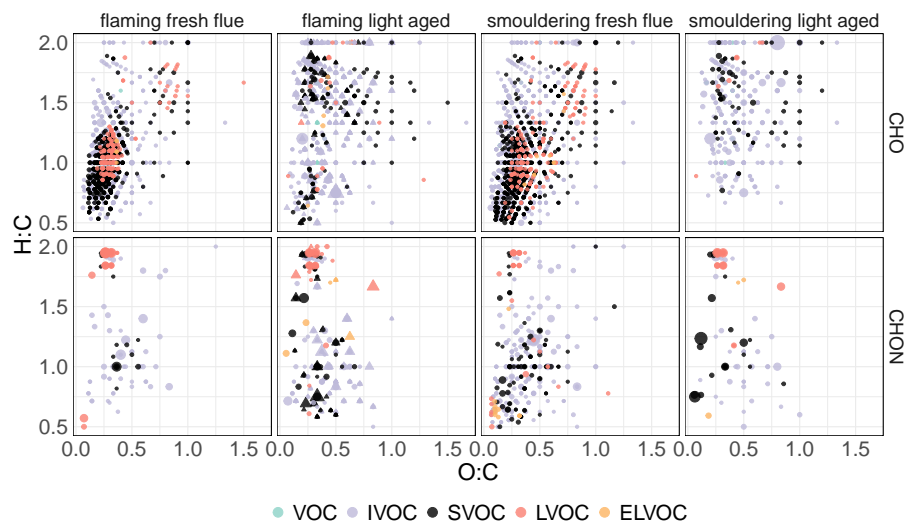
Figure A7. Van Krevelen diagrams of H:C and O:C ratios for CHO (top row) and CHON (bottom row) compounds in the OA derived from flaming dominated and smouldering dominated burn phases. In the flaming light aged panel the point shape represents the two repeats: FL_AGED_1 (circles) and FL_AGED_2 (triangles). Compounds are coloured by the volatility estimations described in the Li et al. (2016) parameterisation for volatile organic compounds (VOC), intermediate volatile organic compounds (IVOC), semi-volatile organic compounds (SVOC), low volatile organic compounds (LVOC) and extremely low volatile organic compounds (ELVOC)

References

Adler, G., Flores, J. M., Riziq, A. A., Borrmann, S., and Rudich, Y.: Chemical, physical, and optical evolution of biomass burning aerosols: a case study, Atmos. Chem. Phys, 11, 1491–1503, https://doi.org/10.5194/acp-11-1491-2011, 2011.

Akherati, A., He, Y., Coggon, M. M., Koss, A. R., Hodshire, A. L., Sekimoto, K., Warneke, C., Gouw, J. D., Yee, L., Seinfeld, J. H., Onasch, T. B., Herndon, S. C., Knighton, W. B., Cappa, C. D., Kleeman, M. J., Lim, C. Y., Kroll, J. H., Pierce, J. R., and Jathar, S. H.: Oxygenated Aromatic Compounds are Important Precursors of Secondary Organic Aerosol in Biomass-Burning Emissions, Environ. Sci. Technol., 54, 8568–8579, https://doi.org/10.1021/acs.est.0c01345, 2020.

Allan, J. D., Williams, P. I., Morgan, W. T., Martin, C. L., Flynn, M. J., Lee, J., Nemitz, E., Phillips, G. J., Gallagher, M. W., and Coe, H.: Contributions from transport, solid fuel burning and cooking to primary organic aerosols in two UK cities, Atmos. Chem. Phys, 10, 647–668, https://doi.org/10.5194/acp-10-647-2010, 2010.

An, Y., Xu, J., Feng, L., Zhang, X., Liu, Y., Kang, S., Jiang, B., and Liao, Y.: Molecular characterization of organic aerosol in the Himalayas: insight from ultra-high-resolution mass spectrometry, Atmos. Chem. Phys., 19, 1115–1128, https://doi.org/10.5194/acp-19-1115-2019, 2019.

Andreae, M. O.: Emission of trace gases and aerosols from biomass burning – an updated assessment, Atmos. Chem. Phys., 19, 8523–8546, https://doi.org/10.5194/acp-19-8523-2019, 2019.

Andreae, M. O. and Merlet, P.: Emission of trace gases and aerosols from biomass burning, Glob. Biogeochem. Cycles, 15, 955–966, https://doi.org/10.1029/2000GB001382, 2001.

Andrew Price-Allison, Jenny Jones, A. W.: Future Fuels Report, Tech. rep., Department for Environment Food Rural Affairs, 2022.

Bertrand, A., Stefenelli, G., Bruns, E. A., Pieber, S. M., Temime-Roussel, B., Slowik, J. G., Prévôt, A. S., Wortham, H., Haddad, I. E., and Marchand, N.: Primary emissions and secondary aerosol production potential from woodstoves for residential heating: Influence of the stove technology and combustion efficiency, Atmos. Environ., 169, 65–79, https://doi.org/10.1016/J.ATMOSENV.2017.09.005, 2017.

Bertrand, A., Stefenelli, G., Jen, C. N., Pieber, S. M., Bruns, E. A., Ni, H., Temime-Roussel, B., Slowik, J. G., Goldstein, A. H., Haddad, I. E., Baltensperger, U., Prévôt, A. S., Wortham, H., and Marchand, N.: Evolution of the chemical fingerprint of biomass burning organic aerosol during aging, Atmos. Chem. Phys., 18, 7607–7624, https://doi.org/10.5194/acp-18-7607-2018, 2018.

Bloss, C., Wagner, V., Bonzanini, A., Jenkin, M. E., Wirtz, K., Martin-Reviejo, M., and Pilling, M. J.: Evaluation of detailed aromatic mechanisms (MCMv3 and MCMv3.1) against environmental chamber data, Atmos. Chem. Phys, 5, 623–639, https://doi.org/10.5194/acp-5-623-2005, 2005.

Brege, M., Paglione, M., Gilardoni, S., Decesari, S., Facchini, M. C., and Mazzoleni, L. R.: Molecular insights on aging and aqueous-phase processing from ambient biomass burning emissions-influenced Po Valley fog and aerosol, Atmos. Chem. Phys., 18, 13 197–13 214, https://doi.org/10.5194/acp-18-13197-2018, 2018.

Brege, M. A., China, S., Schum, S., Zelenyuk, A., and Mazzoleni, L. R.: Extreme Molecular Complexity Resulting in a Continuum of Carbonaceous Species in Biomass Burning Tar Balls from Wildfire Smoke, ACS Earth Space Chem., 5, 2729–2739, https://doi.org/10.1021/ACSEARTHSPACECHEM.1C00141, 2021.

Bruns, E. A., Krapf, M., Orasche, J., Huang, Y., Zimmermann, R., Drinovec, L., Močnik, G., El-Haddad, I., Slowik, J. G., Dommen, J., Baltensperger, U., and Prévôt, A. S. H.: Characterization of primary and secondary wood combustion products generated under different burner loads, Atmos. Chem. Phys, 15, 2825–2841, https://doi.org/10.5194/acp-15-2825-2015, 2015.

Bryant, D. J., Mayhew, A. W., Pereira, K. L., Budisulistiorini, S. H., Prior, C., Unsworth, W., Topping, D. O., Rickard, A. R., and Hamilton, J. F.: Overcoming the lack of authentic standards for the quantification of biogenic secondary organic aerosol markers, Environ. Sci.: Atmos., 3, 221–229, https://doi.org/10.1039/D2EA00074A, 2023.

610 Budisulistiorini, S. H., Riva, M., Williams, M., Chen, J., Itoh, M., Surratt, J. D., and Kuwata, M.: Light-Absorbing Brown Carbon Aerosol Constituents from Combustion of Indonesian Peat and Biomass, Environ. Sci. Technol., 51, 4415–4423, https://doi.org/10.1021/acs.est.7b00397, 2017.

Budisulistiorini, S. H., Chen, J., Itoh, M., and Kuwata, M.: Can Online Aerosol Mass Spectrometry Analysis Classify Secondary Organic Aerosol (SOA) and Oxidized Primary Organic Aerosol (OPOA)? A Case Study of Laboratory and Field Studies of Indonesian Biomass

615 Burning, ACS Earth and Space Chemistry, 5, 3511–3522, https://doi.org/10.1021/acsearthspacechem.1c00319, 2021.

Cai, D., Wang, X., George, C., Cheng, T., Herrmann, H., Li, X., and Chen, J.: Formation of Secondary Nitroaromatic Compounds in Polluted Urban Environments, J. Geophys. Res.: Atmos., 127, e2021JD036 167, https://doi.org/10.1029/2021JD036167, 2022.

Capes, G., Johnson, B., McFiggans, G., Williams, P. I., Haywood, J., and Coe, H.: Aging of biomass burning aerosols over West Africa: Aircraft measurements of chemical composition, microphysical properties, and emission ratios, J. Geophys. Res. Atmos., 113,

620 https://doi.org/10.1029/2008JD009845, 2008.

Casey, J., Mittal, L., Buchanan, L., Fuller, G., and Mead, I.: London wood burning project: air quality data collection, Tech. rep., Environmental Research Group, Imperial College London, 2023.

Chen, L., Bao, Z., Wu, X., Li, K., Han, L., Zhao, X., Zhang, X., Wang, Z., Azzi, M., and Cen, K.: The effects of humidity and ammonia on the chemical composition of secondary aerosols from toluene/NOx photo-oxidation, Sci. Tot. Environ., 728, 138 671,

625 https://doi.org/10.1016/J.SCITOTENV.2020.138671, 2020.

Chen, T., Chu, B., Ma, Q., Zhang, P., Liu, J., and He, H.: Effect of relative humidity on SOA formation from aromatic hydrocarbons: Implications from the evolution of gas- and particle-phase species, Sci. Tot. Environ., 773, 145 015, https://doi.org/10.1016/J.SCITOTENV.2021.145015, 2021.

Chhabra, P. S., Flagan, R. C., and Seinfeld, J. H.: Elemental analysis of chamber organic aerosol using an aerodyne high-resolution aerosol

630 mass spectrometer, Atmos. Chem. Phys., 10, 4111–4131, https://doi.org/10.5194/acp-10-4111-2010, 2010.

Claeys, M., Vermeylen, R., Yasmeen, F., Gómez-González, Y., Chi, X., Maenhaut, W., Mészáros, T., and Salma, I.: Chemical characterisation of humic-like substances from urban, rural and tropical biomass burning environments using liquid chromatography with UV/vis photodiode array detection and electrospray ionisation mass spectrometry, Environ. Chem., 9, 273, https://doi.org/10.1071/EN11163, 2012.

Cubison, M. J., Ortega, A. M., Hayes, P. L., Farmer, D. K., Day, D., Lechner, M. J., Brune, W. H., Apel, E., Diskin, G. S., Fisher, J. A.,

635 Fuelberg, H. E., Hecobian, A., Knapp, D. J., Mikoviny, T., Riemer, D., Sachse, G. W., Sessions, W., Weber, R. J., Weinheimer, A. J., Wisthaler, A., and Jimenez, J. L.: Effects of aging on organic aerosol from open biomass burning smoke in aircraft and laboratory studies, Atmos. Chem. Phys, 11, 12 049–12 064, https://doi.org/10.5194/acp-11-12049-2011, 2011.

Czech, H., Sippula, O., Kortelainen, M., Tissari, J., Radischat, C., Passig, J., Streibel, T., Jokiniemi, J., and Zimmermann, R.: On-line analysis of organic emissions from residential wood combustion with single-photon ionisation time-of-flight mass spectrometry (SPI-TOFMS),

640 Fuel, 177, 334–342, https://doi.org/10.1016/J.FUEL.2016.03.036, 2016.

Daellenbach, K. R., Kourtchev, I., Vogel, A. L., Bruns, E. A., Jiang, J., Petäjä, T., Jaffrezo, J.-L., Aksoyoglu, S., Kalberer, M., Baltensperger, U., Haddad, I. E., and Prévôt, A. S. H.: Impact of anthropogenic and biogenic sources on the seasonal variation in the molecular composition of urban organic aerosols: a field and laboratory study using ultra-high-resolution mass spectrometry, Atmos. Chem. Phys., 19, 5973–5991, https://doi.org/10.5194/acp-19-5973-2019, 2019.

645 Delmas, R., Lacaux, J. P., Menaut, J. C., Abbadie, L., Roux, X. L., Helas, G., and Lobert, J.: Nitrogen compound emission from biomass burning in tropical African savanna FOS/DECAFE 1991 experiment (Lamto, Ivory Coast), J. Atmos. Chem., 22, 175–193, https://doi.org/10.1007/BF00708188, 1995.

Department for Environment Food & Rural Affairs (DEFRA): Burning in UK Homes and Gardens Research Report, Tech. rep., DEFRA, 2020.

650 Desyaterik, Y., Sun, Y., Shen, X., Lee, T., Wang, X., Wang, T., and Collett, J. L.: Speciation of "brown" carbon in cloud water impacted by agricultural biomass burning in eastern China, J. Geophys. Res.: Atmos., 118, 7389–7399, https://doi.org/10.1002/JGRD.50561, 2013.

Dzepina, K., Mazzoleni, C., Fialho, P., China, S., Zhang, B., Owen, R. C., Helmig, D., Hueber, J., Kumar, S., Perlinger, J. A., Kramer, L. J., Dziobak, M. P., Ampadu, M. T., Olsen, S., Wuebbles, D. J., and Mazzoleni, L. R.: Molecular characterization of free tropospheric aerosol collected at the Pico Mountain Observatory: A case study with a long-range transported biomass burning plume, Atmos. Chem. Phys., 15, 655 5047–5068, https://doi.org/10.5194/acp-15-5047-2015, 2015.

Evans, R., Bryant, D., Voliotis, A., Hu, D., Wu, H., Syafira, S., Oghama, O., McFiggans, G., Hamilton, J., and Rickard, A.: A Semi-Quantitative Approach to Nontarget Compositional Analysis of Complex Samples, Anal. Chem., 96, 18 349–18 358, https://doi.org/10.1021/acs.analchem.4c00819, 2024.

Fang, Z., Li, C., He, Q., Czech, H., Gröger, T., Zeng, J., Fang, H., Xiao, S., Pardo, M., Hartner, E., Meidan, D., Wang, X., Zim- 660 mermann, R., Laskin, A., and Rudich, Y.: Secondary organic aerosols produced from photochemical oxidation of secondarily evaporated biomass burning organic gases: Chemical composition, toxicity, optical properties, and climate effect, Environ. Int., 157, https://doi.org/10.1016/j.envint.2021.106801, 2021.

Fitzpatrick, E. M., Jones, J. M., Pourkashanian, M., Ross, A. B., Williams, A., and Bartle, K. D.: Mechanistic aspects of soot formation from the combustion of pine wood, Energy Fuels, 22, 3771–3778, https://doi.org/10.1021/EF800456K, 2008.

665 Fleming, L. T., Lin, P., Roberts, J. M., Selimovic, V., Yokelson, R., Laskin, J., Laskin, A., and Nizkorodov, S. A.: Molecular composition and photochemical lifetimes of brown carbon chromophores in biomass burning organic aerosol, Atmos. Chem. Phys., 20, 1105–1129, https://doi.org/10.5194/acp-20-1105-2020, 2020.

Gilardoni, S., Massoli, P., Paglione, M., Giulianelli, L., Carbone, C., Rinaldi, M., Decesari, S., Sandrini, S., Costabile, F., Gobbi, G. P., Pietrogrande, M. C., Visentin, M., Scotto, F., Fuzzi, S., and Facchini, M. C.: Direct observation of aqueous secondary organic aerosol 670 from biomass-burning emissions, Proc. Natl. Acad. Sci. USA, 113, 10 013–10 018, https://doi.org/10.1073/PNAS.1602212113, 2016.

Gilman, J. B., Lerner, B. M., Kuster, W. C., Goldan, P. D., Warneke, C., Veres, P. R., Roberts, J. M., de Gouw, J. A., Burling, I. R., and Yokelson, R. J.: Biomass burning emissions and potential air quality impacts of volatile organic compounds and other trace gases from fuels common in the US, Atmos. Chem. Phys., 15, 13 915–13 938, https://doi.org/10.5194/acp-15-13915-2015, 2015.

Grieshop, A. P., Logue, J. M., Donahue, N. M., and Robinson, A. L.: Laboratory investigation of photochemical oxidation of or- 675 ganic aerosol from wood fires 1: measurement and simulation of organic aerosol evolution, Atmos. Chem. Phys., 9, 1263–1277, https://doi.org/10.5194/acp-9-1263-2009, 2009.

Guo, J. and Huan, T.: Comparison of Full-Scan, Data-Dependent, and Data-Independent Acquisition Modes in Liquid Chromatography-Mass Spectrometry Based Untargeted Metabolomics, Anal. Chem., 92, 8072–8080, https://doi.org/10.1021/ACS.ANALCHEM.9B05135, 2020.

Herrera-Lopez, S., Hernando, M. D., García-Calvo, E., Fernández-Alba, A. R., and Ulaszewska, M. M.: Simultaneous screening of targeted 680 and nontargeted contaminants using an LC-QTOF-MS system and automated MS/MS library searching, J. Mass Spectrom., 49, 878–893, https://doi.org/10.1002/JMS.3428, 2014.

Iinuma, Y., Brüggemann, E., Gnauk, T., Müller, K., Andreae, M. O., Helas, G., Parmar, R., and Herrmann, H.: Source characterization of biomass burning particles: The combustion of selected European conifers, African hardwood, savanna grass, and German and Indonesian peat, J. Geophys. Res. Atmos., 112, https://doi.org/10.1029/2006JD007120, 2007.

685 Iinuma, Y., Böge, O., and Herrmann, H.: Methyl-nitrocatechols: Atmospheric tracer compounds for biomass burning secondary organic aerosols, Environ. Sci. Technol., 44, 8453–8459, https://doi.org/10.1021/es102938a, 2010.

International Energy Agency: World Energy Outlook 2022, Tech. rep., IEA, www.iea.org/, 2022.

Jen, C. N., Hatch, L. E., Selimovic, V., Yokelson, R. J., Weber, R., Fernandez, A. E., Kreisberg, N. M., Barsanti, K. C., and Goldstein, A. H.: Speciated and total emission factors of particulate organics from burning western US wildland fuels and their dependence on combustion

690 efficiency, Atmos. Chem. Phys, 19, 1013–1026, https://doi.org/10.5194/acp-19-1013-2019, 2019.

Jenkins, B. M., Turn, S. Q., Williams, R. B., Chang, D. P. Y., Raabe, O. G., Paskind, J., and Teague, S.: Quantitative Assessment of Gaseous and Condensed Phase Emissions from Open Burning of Biomass in a Combustion Wind Tunnel, in: Global Biomass Burning: Atmospheric, Climatic, and Biospheric Implications, pp. 305–317, MIT Press, ISBN 9780262310895, 1991.

Jiang, H., Li, J., Chen, D., Tang, J., Cheng, Z., Mo, Y., Su, T., Tian, C., Jiang, B., Liao, Y., and Zhang, G.: Biomass burning organic aerosols

695 significantly influence the light absorption properties of polarity-dependent organic compounds in the Pearl River Delta Region, China, Environ. Int., 144, 106 079, https://doi.org/10.1016/J.ENVINT.2020.106079, 2020.

Jimenez, J. L., Canagaratna, M. R., Donahue, N. M., Prevot, A. S., Zhang, Q., Kroll, J. H., DeCarlo, P. F., Allan, J. D., Coe, H., Ng, N. L., Aiken, A. C., Docherty, K. S., Ulbrich, I. M., Grieshop, A. P., Robinson, A. L., Duplissy, J., Smith, J. D., Wilson, K. R., Lanz, V. A., Hueglin, C., Sun, Y. L., Tian, J., Laaksonen, A., Raatikainen, T., Rautiainen, J., Vaattovaara, P., Ehn, M., Kulmala, M., Tomlinson,

700 J. M., Collins, D. R., Cubison, M. J., Dunlea, E. J., Huffman, J. A., Onasch, T. B., Alfarra, M. R., Williams, P. I., Bower, K., Kondo, Y., Schneider, J., Drewnick, F., Borrmann, S., Weimer, S., Demerjian, K., Salcedo, D., Cottrell, L., Griffin, R., Takami, A., Miyoshi, T., Hatakeyama, S., Shimono, A., Sun, J. Y., Zhang, Y. M., Dzepina, K., Kimmel, J. R., Sueper, D., Jayne, J. T., Herndon, S. C., Trimborn, A. M., Williams, L. R., Wood, E. C., Middlebrook, A. M., Kolb, C. E., Baltensperger, U., and Worsnop, D. R.: Evolution of organic aerosols in the atmosphere, Science, 326, 1525–1529, https://doi.org/10.1126/SCIENCE.1180353, 2009.

705 Jolleys, M. D., Coe, H., Mcfiggans, G., Taylor, J. W., O'shea, S. J., Breton, M. L., Bauguitte, J.-B., Moller, S., Carlo, P. D., Aruffo, E., Palmer, P. I., Lee, J. D., Percival, C. J., and Gallagher, M. W.: Properties and evolution of biomass burning organic aerosol from Canadian boreal forest fires, Atmos. Chem. Phys, 15, 3077–3095, https://doi.org/10.5194/acp-15-3077-2015, 2015.

Kalogridis, A. C., Popovicheva, O. B., Engling, G., Diapouli, E., Kawamura, K., Tachibana, E., Ono, K., Kozlov, V. S., and Eleftheriadis, K.: Smoke aerosol chemistry and aging of Siberian biomass burning emissions in a large aerosol chamber, Atmos. Environ., 185, 15–28,

710 https://doi.org/10.1016/j.atmosenv.2018.04.033, 2018.

Kampa, M. and Castanas, E.: Human health effects of air pollution, Environ. Pollut., 151, 362–367, https://doi.org/10.1016/J.ENVPOL.2007.06.012, 2008.

Kim, Y., Pike, K. A., Gray, R., Sprankle, J. W., Faust, J. A., and Edmiston, P. L.: Non-targeted identification and semi-quantitation of emerging per- and polyfluoroalkyl substances (PFAS) in US rainwater, Environ. Sci.: Process. Impacts., 25, 1771–1787,

715 https://doi.org/10.1039/D2EM00349J, 2023a.

Kim, Y. H., Sinha, A., George, I. J., DeMarini, D. M., Grieshop, A. P., and Gilmour, M. I.: Toxicity of fresh and aged anthropogenic smoke particles emitted from different burning conditions, Sci. Tot. Environ., 892, 164 778, https://doi.org/10.1016/J.SCITOTENV.2023.164778, 2023b.

Kitanovski, Z., Grgić, I., Yasmeen, F., Claeys, M., and Čusak, A.: Development of a liquid chromatographic method based on ultraviolet–visible and electrospray ionization mass spectrometric detection for the identification of nitrocatechols and related tracers in biomass burning atmospheric organic aerosol, Rapid Commun. Mass Spectrom., 26, 793–804, https://doi.org/10.1002/RCM.6170, 2012.

Kjällstrand, J. and Olsson, M.: Chimney emissions from small-scale burning of pellets and fuelwood—examples referring to different combustion appliances, Biomass Bioenergy, 27, 557–561, https://doi.org/10.1016/J.BIOMBIOE.2003.08.014, 2004.

Koch, B. P. and Dittmar, T.: From mass to structure: an aromaticity index for high-resolution mass data of natural organic matter, Rapid Communications in Mass Spectrometry, 30, 250–250, https://doi.org/https://doi.org/10.1002/rcm.7433, 2016.

Kourtchev, I., Godoi, R. H. M., Connors, S., Levine, J. G., Archibald, A. T., Godoi, A. F. L., Paralovo, S. L., Barbosa, C. G. G., Souza, R. A. F., Manzi, A. O., Seco, R., Sjostedt, S., Park, J.-H., Guenther, A., Kim, S., Smith, J., Martin, S. T., and Kalberer, M.: Molecular composition of organic aerosols in central Amazonia: an ultra-high-resolution mass spectrometry study, Atmos. Chem. Phys., 16, 11 899–11 913, https://doi.org/10.5194/acp-16-11899-2016, 2016.

Kruve, A., Kiefer, K., and Hollender, J.: Benchmarking of the quantification approaches for the non-targeted screening of micropollutants and their transformation products in groundwater, Anal. Bioanal. Chem., 413, 1549–1559, https://doi.org/10.1007/S00216-020-03109-2, 2021.

Kundu, S., Kawamura, K., Andreae, T. W., Hoffer, A., and Andreae, M. O.: Molecular distributions of dicarboxylic acids, ketocarboxylic acids and α-dicarbonyls in biomass burning aerosols: implications for photochemical production and degradation in smoke layers, Atmos. Chem. Phys, 10, 2209–2225, https://doi.org/10.5194/acp-10-2209-2010, 2010.

Lee, T., Sullivan, A. P., MacK, L., Jimenez, J. L., Kreidenweis, S. M., Onasch, T. B., Worsnop, D. R., Malm, W., Wold, C. E., Hao, W. M., and Collett, J. L.: Chemical smoke marker emissions during flaming and smoldering phases of laboratory open burning of wildland fuels, Aerosol Sci. Technol., 44, https://doi.org/10.1080/02786826.2010.499884, 2010.

Leskinen, J., Tissari, J., Uski, O., Virén, A., Torvela, T., Kaivosoja, T., Lamberg, H., Nuutinen, I., Kettunen, T., Joutsensaari, J., Jalava, P. I., Sippula, O., Hirvonen, M. R., and Jokiniemi, J.: Fine particle emissions in three different combustion conditions of a wood chip-fired appliance – Particulate physico-chemical properties and induced cell death, Atmos. Environ., 86, 129–139, https://doi.org/10.1016/J.ATMOSENV.2013.12.012, 2014.

Li, J., Li, J., Wang, G., Zhang, T., Dai, W., Ho, K. F., Wang, Q., Shao, Y., Wu, C., and Li, L.: Molecular characteristics of organic compositions in fresh and aged biomass burning aerosols, Sci. Tot. Environ., 741, https://doi.org/10.1016/j.scitotenv.2020.140247, 2020.

Li, S., Liu, D., Hu, D., Kong, S., Wu, Y., Ding, S., Cheng, Y., Qiu, H., Zheng, S., Yan, Q., Zheng, H., Hu, K., Zhang, J., Zhao, D., Liu, Q., Sheng, J., Ye, J., He, H., and Ding, D.: Evolution of Organic Aerosol From Wood Smoke Influenced by Burning Phase and Solar Radiation, J. Geophys. Res., 126, https://doi.org/10.1029/2021JD034534, 2021.

Li, Y., Pöschl, U., and Shiraiwa, M.: Molecular corridors and parameterizations of volatility in the chemical evolution of organic aerosols, Atmos. Chem. Phys., 16, 3327–3344, https://doi.org/10.5194/ACP-16-3327-2016, 2016.

Li, Z., Wen, Q., and Zhang, R.: Sources, health effects and control strategies of indoor fine particulate matter (PM2.5): A review, Sci. Tot. Environ., 586, 610–622, https://doi.org/10.1016/J.SCITOTENV.2017.02.029, 2017.

Liang, Y., Jen, C. N., Weber, R. J., Misztal, P. K., and Goldstein, A. H.: Chemical composition of PM 2.5 in October 2017 Northern California wildfire plumes, Atmos. Chem. Phys, 21, 5719–5737, https://doi.org/10.5194/acp-21-5719-2021, 2021.

Liang, Y., Stamatis, C., Fortner, E. C., Wernis, R. A., Rooy, P. V., Majluf, F., Yacovitch, T. I., Daube, C., Herndon, S. C., Kreisberg, N. M., Barsanti, K. C., and Goldstein, A. H.: Emissions of organic compounds from western US wildfires and their near-fire transformations, Atmos. Chem. Phys, 22, 9877–9893, https://doi.org/10.5194/acp-22-9877-2022, 2022.

Liigand, P., Liigand, J., Kaupmees, K., and Kruve, A.: 30 Years of research on ESI/MS response: Trends, contradictions and applications, Anal. Chim. Acta, 1152, 238 117, https://doi.org/10.1016/J.ACA.2020.11.049, 2021.

Lin, P., Rincon, A. G., Kalberer, M., and Yu, J. Z.: Elemental composition of HULIS in the Pearl River Delta Region, China: Results inferred from positive and negative electrospray high resolution mass spectrometric data, Environ. Sci. Technol., 46, 7454–7462, https://doi.org/10.1021/es300285d, 2012.

Lin, P., Aiona, P. K., Li, Y., Shiraiwa, M., Laskin, J., Nizkorodov, S. A., and Laskin, A.: Molecular Characterization of Brown Carbon in Biomass Burning Aerosol Particles, Environ. Sci. Technol., 50, 11 815–11 824, https://doi.org/10.1021/acs.est.6b03024, 2016.

Lin, P., Bluvshtein, N., Rudich, Y., Nizkorodov, S. A., Laskin, J., and Laskin, A.: Molecular Chemistry of Atmospheric Brown Carbon Inferred from a Nationwide Biomass Burning Event, Environ. Sci. Technol., 51, 11 561–11 570, https://doi.org/10.1021/acs.est.7b02276, 2017.

Liu, W. J., Li, W. W., Jiang, H., and Yu, H. Q.: Fates of Chemical Elements in Biomass during Its Pyrolysis, Chem. Rev., 117, 6367–6398, https://doi.org/10.1021/acs.chemrev.6b00647, 2017.

Lobert, J. M. and Warnatz, J.: Emissions from the combustion process in vegetation, in: Fire in the Environment: The Ecological, Atmospheric, and Climatic Importance of Vegetation Fires, pp. 15–37, John Wiley & Sons Ltd, 1993.

Loza, C. L., Chhabra, P. S., Yee, L. D., Craven, J. S., Flagan, R. C., and Seinfeld, J. H.: Chemical aging of m-xylene secondary organic aerosol: laboratory chamber study, Atmos. Chem. Phys., 12, 151–167, https://doi.org/10.5194/acp-12-151-2012, 2012.

Mayhew, A. W., Topping, D. O., and Hamilton, J. F.: New Approach Combining Molecular Fingerprints and Machine Learning to Estimate Relative Ionization Efficiency in Electrospray Ionization, ACS Omega, 5, 9510–9516, https://doi.org/10.1021/ACSOMEGA.0C00732, 2020.

McDuffie, E. E., Martin, R. V., Spadaro, J. V., Burnett, R., Smith, S. J., O'Rourke, P., Hammer, M. S., van Donkelaar, A., Bindle, L., Shah, V., Jaeglé, L., Luo, G., Yu, F., Adeniran, J. A., Lin, J., and Brauer, M.: Source sector and fuel contributions to ambient PM2.5 and attributable mortality across multiple spatial scales, Nat. Commun., 12, 1–12, https://doi.org/10.1038/s41467-021-23853-y, 2021.

Ofner, J., Krüger, H.-U., Grothe, H., Schmitt-Kopplin, P., Whitmore, K., and Zetzsch, C.: Physico-chemical characterization of SOA derived from catechol and guaiacol – a model substance for the aromatic fraction of atmospheric HULIS, Atmos. Chem. Phys., 11, 1–15, https://doi.org/10.5194/acp-11-1-2011, 2011.

Oppenheimer, C., Tsanev, V. I., Allen, A. G., McGonigle, A. J., Cardoso, A. A., Wiatr, A., Paterlini, W., and Dias, C. D. M.: NO2 emissions from agricultural burning in São Paulo, Brazil, Environ. Sci. Technol., 38, 4557–4561, https://doi.org/10.1021/ES0496219, 2004.

Orasche, J., Schnelle-Kreis, J., Schön, C., Hartmann, H., Ruppert, H., Arteaga-Salas, J. M., and Zimmermann, R.: Comparison of emissions from wood combustion. Part 2: Impact of combustion conditions on emission factors and characteristics of particle-bound organic species and polycyclic aromatic hydrocarbon (PAH)-related toxicological potential, Energy Fuels, 27, 1482–1491, https://doi.org/10.1021/EF301506H, 2013.

Oss, M., Kruve, A., Herodes, K., and Leito, I.: Electrospray Ionization Efficiency Scale of Organic Compounds, Anal. Chem., 82, 2865–2872, https://doi.org/10.1021/ac902856t, 2010.

Pereira, K. L., Ward, M. W., Wilkinson, J. L., Sallach, J. B., Bryant, D. J., Dixon, W. J., Hamilton, J. F., and Lewis, A. C.: An Automated Methodology for Non-targeted Compositional Analysis of Small Molecules in High Complexity Environmental Matrices Using Coupled Ultra Performance Liquid Chromatography Orbitrap Mass Spectrometry, Environ. Sci. Technol., 55, 7365–7375, https://doi.org/10.1021/acs.est.0c08208, 2021.

Pieke, E. N., Granby, K., Trier, X., and Smedsgaard, J.: A framework to estimate concentrations of potentially unknown substances by semi-quantification in liquid chromatography electrospray ionization mass spectrometry, Anal. Chim. Acta, 975, 30–41, https://doi.org/10.1016/J.ACA.2017.03.054, 2017.

Piot, C., Jaffrezo, J.-L., Cozic, J., Pissot, N., Haddad, I. E., Marchand, N., and Besombes, J.-L.: Quantification of levoglucosan and its isomers by High Performance Liquid Chromatography – Electrospray Ionization tandem Mass Spectrometry and its applications to atmospheric and soil samples, Atmos. Meas. Tech., 5, 141–148, https://doi.org/10.5194/amt-5-141-2012, 2012.

Pluskal, T., Castillo, S., Villar-Briones, A., and Orešič, M.: MZmine 2: Modular framework for processing, visualizing, and analyzing mass spectrometry-based molecular profile data, BMC Bioinformatics, 11, 1–11, https://doi.org/10.1186/1471-2105-11-395, 2010.

Qi, L., Chen, M., Stefenelli, G., Pospisilova, V., Tong, Y., Bertrand, A., Hueglin, C., Ge, X., Baltensperger, U., Prévôt, A. S. H., and Slowik, J. G.: Organic aerosol source apportionment in Zurich using an extractive electrospray ionization time-of-flight mass spectrometer (EESI-TOF-MS) – Part 2: Biomass burning influences in winter, Atmos. Chem. Phys., 19, 8037–8062, https://doi.org/10.5194/acp-19-8037-2019, 2019.

Rattanavaraha, W., Chu, K., Budisulistiorini, S. H., Riva, M., Lin, Y.-H., Edgerton, E. S., Baumann, K., Shaw, S. L., Guo, H., King, L., Weber, R. J., Neff, M. E., Stone, E. A., Offenberg, J. H., Zhang, Z., Gold, A., and Surratt, J. D.: Assessing the impact of anthropogenic pollution on isoprene-derived secondary organic aerosol formation in PM 2.5 collected from the Birmingham, Alabama, ground site during the 2013 Southern Oxidant and Aerosol Study, Atmos. Chem. Phys, 16, 4897–4914, https://doi.org/10.5194/acp-16-4897-2016, 2016.

Roberts, J. M., Stockwell, C. E., Yokelson, R. J., Gouw, J. D., Liu, Y., Selimovic, V., Koss, A. R., Sekimoto, K., Coggon, M. M., Yuan, B., Zarzana, K. J., Brown, S. S., Santin, C., Doerr, S. H., and Warneke, C.: The nitrogen budget of laboratory-simulated western US wildfires during the FIREX 2016 Fire Lab study, Atmos. Chem. Phys, 20, 8807–8826, https://doi.org/10.5194/acp-20-8807-2020, 2020.

Schmid, R., Heuckeroth, S., Korf, A., Smirnov, A., Myers, O., Dyrlund, T. S., Bushuiev, R., Murray, K. J., Hoffmann, N., Lu, M., Sarvepalli, A., Zhang, Z., Fleischauer, M., Dührkop, K., Wesner, M., Hoogstra, S. J., Rudt, E., Mokshyna, O., Brungs, C., Ponomarov, K., Mutabdžija, L., Damiani, T., Pudney, C. J., Earll, M., Helmer, P. O., Fallon, T. R., Schulze, T., Rivas-Ubach, A., Bilbao, A., Richter, H., Nothias, L. F., Wang, M., Orešič, M., Weng, J. K., Böcker, S., Jeibmann, A., Hayen, H., Karst, U., Dorrestein, P. C., Petras, D., Du, X., and Pluskal, T.: Integrative analysis of multimodal mass spectrometry data in MZmine 3, Nature Biotechnology 2023 41:4, 41, 447–449, https://doi.org/10.1038/s41587-023-01690-2, 2023.

Sekimoto, K., Koss, A. R., Gilman, J. B., Selimovic, V., Coggon, M. M., Zarzana, K. J., Yuan, B., Lerner, B. M., Brown, S. S., Warneke, C., Yokelson, R. J., Roberts, J. M., and de Gouw, J.: High- and low-temperature pyrolysis profiles describe volatile organic compound emissions from western US wildfire fuels, Atmos. Chem. Phys., 18, 9263–9281, https://doi.org/10.5194/acp-18-9263-2018, 2018.

Sepman, H., Malm, L., Peets, P., Macleod, M., Martin, J., Breitholtz, M., and Kruve, A.: Bypassing the Identification: MS2Quant for Concentration Estimations of Chemicals Detected with Nontarget LC-HRMS from MS 2 Data, Anal. Chem., 95, 12 329–12 338, https://doi.org/10.1021/acs.analchem.3c01744, 2023.

Shafizadeh, F.: Introduction to pyrolysis of biomass, J. Anal. Appl. Pyrolysis, 3, 283–305, https://doi.org/10.1016/0165-2370(82)80017-X, 1982.

Shao, Y., Wang, Y., Du, M., Voliotis, A., Alfarra, M. R., O'Meara, S. P., Turner, S. F., and McFiggans, G.: Characterisation of the Manchester Aerosol Chamber facility, Atmos. Meas. Tech., 15, 539–559, https://doi.org/10.5194/amt-15-539-2022, 2022.

Simoneit, B. R.: Biomass burning — a review of organic tracers for smoke from incomplete combustion, Appl. Geochem., 17, 129–162, https://doi.org/10.1016/S0883-2927(01)00061-0, 2002.

Simoneit, B. R. T., Rogge, W. F., Mazurek, M. A., Standley, L. J., Hlldemann, L. M., and Cass, G. R.: Lignin Pyrolysis Products, Lignans, and Resin Acids as Specific Tracers of Plant Classes in Emissions from Biomass Combustion, Environ. Sci. Technol., 27, 2533–2541, https://doi.org/10.1021/es00048a034, 1993.

835 Smith, D. M., Cui, T., Fiddler, M. N., Pokhrel, R. P., Surratt, J. D., and Bililign, S.: Laboratory studies of fresh and aged biomass burning aerosol emitted from east African biomass fuels-Part 2: Chemical properties and characterization, Atmos. Chem. Phys., 20, 10 169–10 191, https://doi.org/10.5194/acp-20-10169-2020, 2020.

Smith, J. S., Laskin, A., and Laskin, J.: Molecular characterization of biomass burning aerosols using high-resolution mass spectrometry, Anal. Chem., 81, 1512–1521, https://doi.org/10.1021/AC8020664, 2009.

Stefenelli, G., Jiang, J., Bertrand, A., Bruns, E. A., Pieber, S. M., Baltensperger, U., Marchand, N., Aksoyoglu, S., Prévôt, A. S. H.,
840 Slowik, J. G., and Haddad, I. E.: Secondary organic aerosol formation from smoldering and flaming combustion of biomass: a box model parametrization based on volatility basis set, Atmos. Chem. Phys., 19, 11 461–11 484, https://doi.org/10.5194/acp-19-11461-2019, 2019.

Stewart, G. J., Acton, W. J. F., Nelson, B. S., Vaughan, A. R., Hopkins, J. R., Arya, R., Mondal, A., Jangirh, R., Ahlawat, S., Yadav, L., Sharma, S. K., Dunmore, R. E., Yunus, S. S., Hewitt, C. N., Nemitz, E., Mullinger, N., Gadi, R., Sahu, L. K., Tripathi, N., Rickard, A. R.,
845 Lee, J. D., Mandal, T. K., and Hamilton, J. F.: Emissions of non-methane volatile organic compounds from combustion of domestic fuels in Delhi, India, Atmos. Chem. Phys., 21, 2383–2406, https://doi.org/10.5194/acp-21-2383-2021, 2021.

Tasoglou, A., Saliba, G., Subramanian, R., and Pandis, S. N.: Absorption of chemically aged biomass burning carbonaceous aerosol, J. Aerosol Sci., 113, 141–152, https://doi.org/10.1016/J.JAEROSCI.2017.07.011, 2017.

Voliotis, A., Wang, Y., Shao, Y., Du, M., Bannan, T. J., Percival, C. J., Pandis, S. N., Alfarra, M. R., and Mcfiggans, G.: Exploring the
850 composition and volatility of secondary organic aerosols in mixed anthropogenic and biogenic precursor systems, Atmos. Chem. Phys, 21, 14 251–14 273, https://doi.org/10.5194/acp-21-14251-2021, 2021.

Voliotis, A., Du, M., Wang, Y., Shao, Y., Alfarra, M. R., Bannan, T. J., Hu, D., Pereira, K. L., Hamilton, J. F., Hallquist, M., Mentel, T. F., and Mcfiggans, G.: Chamber investigation of the formation and transformation of secondary organic aerosol in mixtures of biogenic and anthropogenic volatile organic compounds, Atmos. Chem. Phys, 22, 14 147–14 175, https://doi.org/10.5194/acp-22-14147-2022, 2022a.

855 Voliotis, A., Du, M., Wang, Y., Shao, Y., Bannan, T. J., Flynn, M., Pandis, S. N., Percival, C. J., Alfarra, M. R., and McFiggans, G.: The influence of the addition of isoprene on the volatility of particles formed from the photo-oxidation of anthropogenic–biogenic mixtures, Atmos.Chem. Phys, 22, 13 677–13 693, https://doi.org/10.5194/acp-22-13677-2022, 2022b.

Wang, X., Hayeck, N., Brüggemann, M., Yao, L., Chen, H., Zhang, C., Emmelin, C., Chen, J., George, C., and Wang, L.: Chemical Characteristics of Organic Aerosols in Shanghai: A Study by Ultrahigh-Performance Liquid Chromatography Coupled With Orbitrap Mass
860 Spectrometry, J. Geophys. Res.: Atmos., 122, 11,703–11,722, https://doi.org/10.1002/2017JD026930, 2017a.

Wang, X., Hayeck, N., Brüggemann, M., Abis, L., Riva, M., Lu, Y., Wang, B., Chen, J., George, C., and Wang, L.: Chemical Characteristics and Brown Carbon Chromophores of Atmospheric Organic Aerosols Over the Yangtze River Channel: A Cruise Campaign, J. Geophys. Res.: Atmos., 125, https://doi.org/10.1029/2020JD032497, 2020.

Wang, Y., Hu, M., Lin, P., Guo, Q., Wu, Z., Li, M., Zeng, L., Song, Y., Zeng, L., Wu, Y., Guo, S., Huang, X., and He, L.: Molecular
865 Characterization of Nitrogen-Containing Organic Compounds in Humic-like Substances Emitted from Straw Residue Burning, Environ. Sci. Technol., 51, 5951–5961, https://doi.org/10.1021/acs.est.7b00248, 2017b.

Wang, Y., Liang, S., Breton, M. L., Wang, Q. Q., Liu, Q., Ho, C. H., Kuang, B. Y., Wu, C., Hallquist, M., Tong, R., and Yu, J. Z.: Field observations of C2 and C3 organosulfates and insights into their formation mechanisms at a suburban site in Hong Kong, Sci. Tot. Environ., 904, 166 851, https://doi.org/10.1016/J.SCITOTENV.2023.166851, 2023.

870 Wang, Z., Zhang, J., Zhang, L., Liang, Y., and Shi, Q.: Characterization of nitroaromatic compounds in atmospheric particulate matter from Beijing, Atmos. Environ., 246, 118 046, https://doi.org/10.1016/J.ATMOSENV.2020.118046, 2021.

Wang, Z., Ge, Y., Bi, S., Liang, Y., and Shi, Q.: Molecular characterization of organic aerosol in winter from Beijing using UHPLC-Orbitrap MS, Sci. Tot. Environ., 812, https://doi.org/10.1016/j.scitotenv.2021.151507, 2022.

Ward, T. J., Semmens, E. O., Weiler, E., Harrar, S., and Noonan, C. W.: Efficacy of interventions targeting household air pollution from
875 residential wood stoves, J. Expo. Sci Environ. Epidemiol., 27, 64–71, https://doi.org/10.1038/jes.2015.73, 2015.

Weimer, S., Alfarra, M. R., Schreiber, D., Mohr, M., Prévôt, A. S., and Baltensperger, U.: Organic aerosol mass spectral signatures from wood-burning emissions: Influence of burning conditions and wood type, J. Geophys. Res.: Atmos., 113, 10 304, https://doi.org/10.1029/2007JD009309, 2008.

World Bank: Tracking SDG 7: The Energy Progress Report 2024, Tech. rep., IEA, IRENA, WHO, United Nations Statistics Division, World
880 Bank, www.worldbank.org, 2024.

World Health Organisation (WHO): Household air pollution, https://www.who.int/news-room/fact-sheets/detail/household-air-pollution-and-health, accessed on 2024-08-21, 2022.

Young, D. E., Allan, J. D., Williams, P. I., Green, D. C., Harrison, R. M., Yin, J., Flynn, M. J., Gallagher, M. W., and Coe, H.: Investigating a two-component model of solid fuel organic aerosol in London: processes, PM 1 contributions, and seasonality, Atmos. Chem. Phys, 15,
885 2429–2443, https://doi.org/10.5194/acp-15-2429-2015, 2015.

Zangrando, R., Barbaro, E., Zennaro, P., Rossi, S., Kehrwald, N. M., Gabrieli, J., Barbante, C., and Gambaro, A.: Molecular Markers of Biomass Burning in Arctic Aerosols, Environ. Sci. Technol., 47, 8565–8574, https://doi.org/10.1021/es400125r, 2013.

Zhang, J., Liu, D., Kong, S., Wu, Y., Li, S., Hu, D., Hu, K., Ding, S., Qiu, H., Li, W., and Liu, Q.: Contrasting resistance of polycyclic aromatic hydrocarbons to atmospheric oxidation influenced by burning conditions, Environ. Res., 211, 113 107,
890 https://doi.org/10.1016/J.ENVRES.2022.113107, 2022.

Zhang, X., Lin, Y. H., Surratt, J. D., and Weber, R. J.: Sources, composition and absorption Ångström exponent of light-absorbing organic components in aerosol extracts from the los angeles basin, Environ. Sci. Technol., 47, 3685–3693, https://doi.org/10.1021/ES305047B, 2013.

Zhou, Y., West, C. P., Hettiyadura, A. P., Pu, W., Shi, T., Niu, X., Wen, H., Cui, J., Wang, X., and Laskin, A.: Molecular Characterization
895 of Water-Soluble Brown Carbon Chromophores in Snowpack from Northern Xinjiang, China, Environ. Sci. Technol., 56, 4173–4186, https://doi.org/10.1021/acs.est.1C07972, 2022.